How wide is the problem? leveraging alternative data sources to enhance channel width representation in watershed modeling

Henrique Haas, Latif Kalin, Enis Baltaci

Highlights

- The default regression equation used in the ArcSWAT program can misrepresent bankfull channel width.
- Bankfull channel width derived from aerial measurements, LiDAR, regional curves, a global database, and a newly developed regression model are tested in the SWAT model.
- The alternative data sources had small impacts on average daily flows but substantial impacts on 1-day maximum flows and water quality simulations.
- Publicly available datasets can be used to enhance channel geometry representation in watershed modeling.

ABSTRACT

Watershed models have been increasingly applied to investigate the impacts of environmental changes on water quantity and quality and to support decision-making. Thus, accurately capturing physical processes and the characteristics of the watershed system is vital to achieving reliable results. Channel geometry features such as cross-sectional shape, bankfull channel width, and depth affect hydraulic parameters like hydraulic radius, wetted perimeter, and cross-sectional area. These, in turn, play important roles in streamflow dynamics, flow velocity, erosion, nutrient transport, and stream ecology. However, the representation of bankfull channel width is often oversimplified in watershed models. Power-law regression equations relating geometric parameters and upstream drainage area are commonly used to calculate bankfull channel width in watershed models. This approach has limitations and may resonate in the misrepresentation of channel geometry with implications for water quantity and quality estimations. This study evaluates how bankfull channel width is represented in a popular watershed model and presents alternative data sources derived from aerial measurements, empirical models, LiDAR, and a global database to mitigate potential misrepresentations. To assess the impacts of bankfull channel width on water quantity and quality, we designed a series of modeling experiments through the Soil and Water Assessment Tool (SWAT) model. We test our methodology in the Alabama-Coosa-Tallapoosa river basin, a large watershed system draining to the Gulf of Mexico coast. Our findings indicate that, overall, the regression equation used in the ArcSWAT program (SWAT's GIS interface) can overestimate bankfull channel width by as much as three times in our study domain. In testing the effects of bankfull width on model simulations we found negligeable implication for water yield predictions. On the other hand, 1-day maximum flows were greatly increased (20%) by using channel width values from the alternative data sources. Simulated water quality was also affected, with stream water temperature showing better agreement with observations under the proposed scenarios. Sediment loadings increased by as much as 118% under the alternative data sources of channel width. Nitrate and phosphate loadings had opposite responses and showed decreases as high as 8.3 and 18.8%, respectively, relative to the default model. Our findings demonstrate that bankfull channel width is misrepresented in watershed models with underlying impacts on simulated water quantity, quality, and ecological flows. Our analysis found bankfull channel width as an important parameter affecting high flows and water quality, and the freely available data sources tested in this study showed good matches with field measurements, making our findings readily available and broadly useful to the modeling community.

KEYWORDS: channel width; watershed modeling; SWAT; water quality modeling; remote-sensing; hydrology

1. **Introduction**

Channel geometry features such as cross-sectional shape, bankfull channel width and depth affect hydraulic parameters like hydraulic radius, wetted perimeter, and cross-sectional area. These variables, in turn, play a crucial role in determining water velocity, volume, sediment, and pollutant transport within the channel, thereby affecting both streamflow and water quality (Choi et al., 2018; Stewardson, 2005). In terms of streamflow, wider channels can mitigate flood risk by accommodating larger water volumes during high-flow events (Kale and Hire, 2004), while narrower channels can increase water flow velocity, leading to increased erosive potential, channel instability, and bank erosion (Fisher et al., 2013; Michalková et al., 2011). In terms of water quality, bankfull width and depth influence the residence time of water and the exchange of water between the channel and surrounding riparian areas, with underlying implications for nutrient cycling and pollutant transport (Baradei, 2020; Sharpley et al., 2013). Additionally, channel geometry shapes aquatic habit distribution, impacting biodiversity and ecosystem functioning (Elosegi et al., 2010; Mac Nally et al., 2011; Rodrigues et al., 2011; Zema et al., 2018). Overall, channel geometric parameters such as bankfull width and depth play an important role in water resources monitoring and hydrologic modeling, as they can have significant impacts on streamflow and water quality.

Hydrologic modeling has become an important approach for understanding and predicting the behavior of water and pollutants in natural systems (Clark et al., 2015; Devia et al., 2015; Guswa et al., 2014). The accuracy of the models depends on a variety of factors, including the bankfull channel width and depth of the system being modeled. Power regression models are commonly used to represent the relationship between channel geometry (e.g., bankfull channel width and depth) and drainage areas in hydrologic models (Ames et al., 2009; Her et al., 2017; Johnson and Fecko, 2008). These models assume a power-law relationship between bankfull width/depth and drainage area, where the geometric parameters increase exponentially with increasing drainage areas (Allen et al., 1994; Bieger et al., 2015; Leopold and Maddock Jr., 1953). This approach is particularly useful for rivers and streams that exhibit a wide range of flow conditions, as it allows for channel width and depth to vary over time as discharge changes.

Such approaches have limitations, particularly in cases where the relationship between channel geometry and drainage area is not well-defined, or where there may be significant variability in the channel geometry due to landscape heterogeneities (Ames et al., 2009; Doll et al., 2002; Her et al., 2017). Also, this simplified method may lead to substantial errors if extrapolated to areas outside the region from which the empirical relationship has been developed. Trapezoidal cross-sectional shapes are commonly used to represent channel geometry in watershed-scale hydrologic models like the National Water Model (NWM) (Gochis et al., 2016), Hydrologic Simulation Program – Fortran (HSPF) (Bicknell et al., 2001), the Soil and Water Assessment Tool (SWAT) model (Arnold et al., 1998), and the *Modelo hidrologico de Grandes Bacias* (MGB) (Collischon et al., 2007). Additionally, these models usually rely on bankfull width and depth values defined by GIS programs based on regression equations. For instance, the HSPF model uses bankfull channel width and depth values determined by BASINS (Better Assessment Science Integrating Point and Nonpoint Sources) (Battin et al., 1998) (Ames et al., 2009). The MGB model relies on bankfull widths and depths calculated by the MGB-IPH Tools/MGB-Preprocessing (Siqueira, et al., 2016) GIS application

(Jardim et al., 2017). Similarly, by default, the SWAT model uses bankfull width and depth values determined by GIS interfaces like ArcSWAT and QSWAT (Han et al., 2019; Her et al., 2017).

Despite the influences of channel geometry on hydrologic fluxes and the increased application of hydrologic models, there is a notable lack of studies assessing the accuracy of channel geometry representation in watershed models and the impacts on simulated water quantity and quality. More recently, there has been growing interest in understanding the effects of channel width and depth on hydrologic modeling. Her et al. (2017) tested ten power-regression equations to estimate channel width and depth in SWAT and their respective impacts on simulated streamflow in a watershed in the Midwest U.S. Results showed small changes in model performance stemming from the different representations of channel geometry. Han et al. (2019) measured channel widths from satellite imagery at sixteen locations across a watershed in South Korea and developed a new power-regression equation for SWAT based on drainage areas. Results demonstrated that the new equation improved model predictions of streamflow, sediments, total nitrogen, and dissolved oxygen. Brackins et al. (2021) assessed the impacts of simple trapezoidal channel geometry representation on the hydrologic predictions of the NWM and proposed alternative approaches based on observed data and two generalized geometries. Results showed that more accurately representing channel geometry led to better stage and discharge predictions. Kim et al. (2022) applied the SWAT model to a small agricultural watershed in South Korea and compared model streamflow predictions under (i) default channel geometry representation, and (ii) measured values at nine locations. The authors demonstrated that by using observed channel widths the model achieved better streamflow performances. While some studies have investigated the effects of channel geometry on specific hydrologic processes, e.g., sediment transport or flow routing, relatively few studies have proposed alternative approaches to generalized regression equations. Factors such as the lack of high-resolution channel width and depth data and the prohibitive costs of large-scale field surveys may have contributed to channel geometry representation being largely overlooked in hydrologic modeling studies. Additionally, because bankfull width and depth are commonly predefined by GIS interfaces, users usually take the default values as ground truth rather than examine them critically.

In recent years, there has been a significant increase in the availability and accessibility of open-source data in Earth System science (Hall et al., 2022; Scanlon et al., 2018; Stagge et al., 2019). This includes remote-sensing technologies, such as satellite imagery, as well as global databases of climate and environmental variables, such as temperature, precipitation, and land cover. Remote-sensing technologies have been widely used to measure channel width and depth in rivers (Allen and Pavelsky, 2018, 2015; Biron et al., 2013; Zheng et al., 2018). One of the commonly used methods is to extract the river centerline from satellite imagery and then calculate the width and depth perpendicular to the centerline (Pavelsky and Smith, 2008). Another approach is to use multispectral imagery to detect changes in color or texture at the water-land interface, which indicates the location of the riverbanks (Leckie et al., 2005; Winterbottom and Gilvear, 1997). Simpler methods like global channel width databases and tools that estimate channel geometry based on water masks, digital elevation models (DEM), and LiDAR (light detection and ranging) technology have also been developed in recent years (Pavelsky and Smith, 2008; Shatnawi and Goodall, 2010; Yamazaki et al., 2014; Yang et al., 2020). However, this valuable information has not been sufficiently explored in hydrologic modeling applications yet.

The overreaching goal of this study is to assess the importance of bankfull channel width representation in current watershed modeling and present alternative resources to enhance it. Using the SWAT model as the modeling tool, we set out to answer the following research questions: (1) How does the default representation of bankfull channel width in the model compare with alternative data sources and field measurments? (2) Can we leverage freely available resources to enhance channel geometry representation in watershed models? (3) What are the effects of channel geometry representation on streamflow and water quality predictions? We test how alternative sources of channel geometry information derived from satellite imagery, empirical models, LiDAR, and global databases affect model performances and simulations. The methodology is tested in a large watershed in Alabama-USA and the impacts on model simulations of streamflow, ecological flows, and stream temperature are assessed across different physiographic regions, drainage areas, land use distributions, stream orders, and elevations. The novelty of this study is in thoroughly evaluating the representation of channel geometry in current watershed modeling and proposing novel and simple approaches to better inform watershed models and enhance their reliability. Our study is the first to leverage publicly available datasets and remote-sensing information to improve the representation of channel geometric parameters in watershed modeling.

2. Methods

2.1.Study domain

The Alabama-Coosa-Tallapoosa (ACT) river basin, which has a drainage area of 59,100 km^2, or 43% of the state of Alabama's surface area, contributes 52% of the water discharged to the Mobile River basin - the fourth largest river basin in North America in terms of flow volume (Johnson et al., 2002). The ACT watershed systems is formed by several smaller watersheds (Figure 1) and spans across parts of Alabama, Georgia, and Mississippi. Given the large geographic extent and importance of the ACT river basin for regional biodiversity, this watershed was selected as a testbed in the current study. Also, there are five different physiographic regions encompassed within the ACT river basin, which makes this watershed an excellent laboratory for assessing how bankfull channel width may impact water quantity and quality across a wide range of physical characteristics (e.g., land-use, soil types, elevation). Physiographic regions are usually strongly linked to stream habitat and biotic life (Goetz and Fiske, 2008; Lenat and Crawford, 1994; Utz et al., 2009). Average elevation ranges from sea level to 1,280 meters in the ACT river basin according to the 30 meters resolution National Elevation Dataset (NED) (NED, 1999). Annual average precipitation and temperature are 1,400 mm and 17 °C, respectively, which characterizes the watershed as a warm and humid system (GridMet database). Rainfall is the main form of precipitation, with evenly distributed amounts over the year, and snowfall is rare, averaging less than 25 mm per year. Soil types across the ACT river basin consist mostly of sandy loam and silty loam whereas forests are the main land cover type.

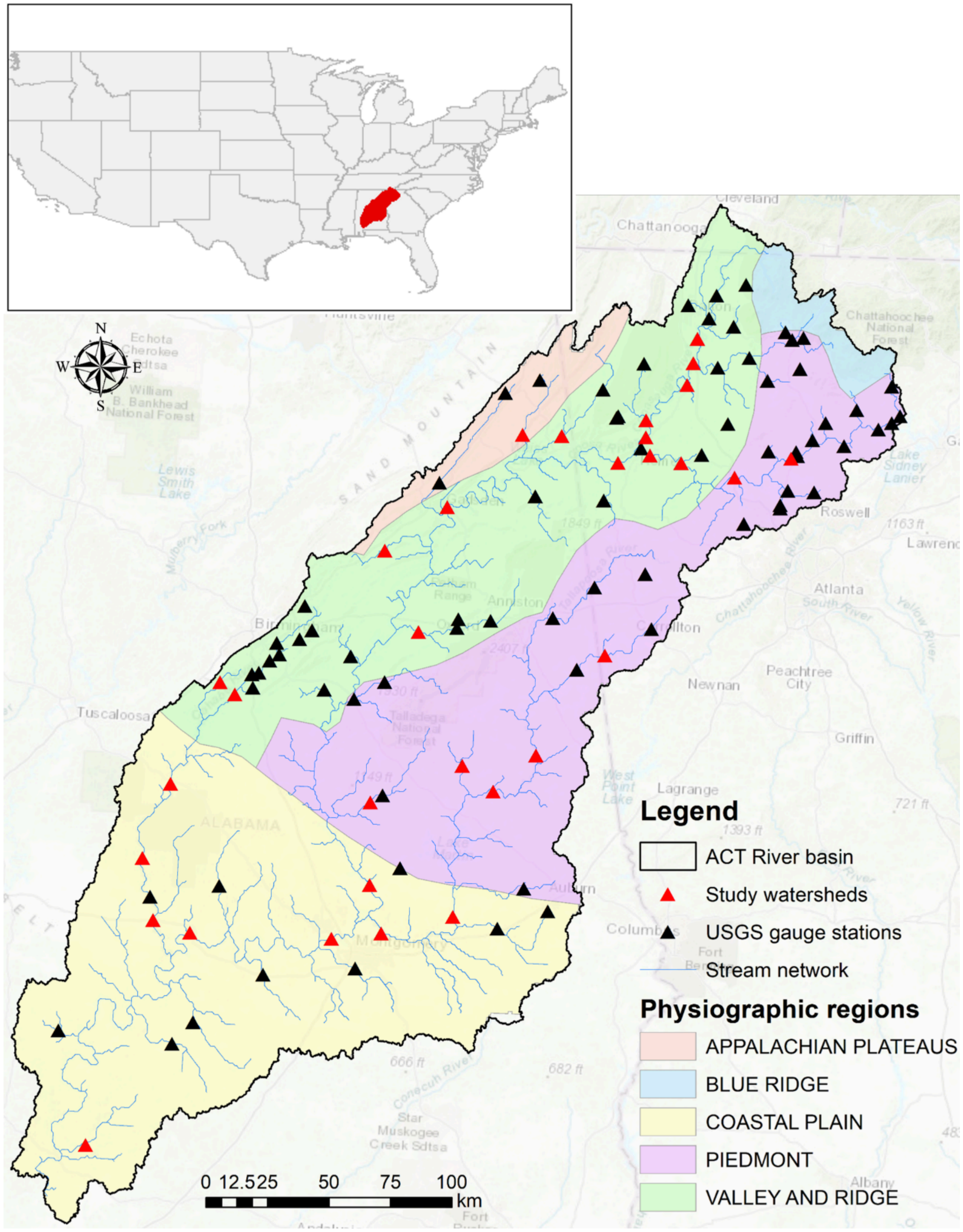

Figure 1 – Location map of the Alabama-Coosa-Tallapoosa (ACT) river basin showing its physiographic regions and the study watersheds where channel width values have been estimated (red triangles). The black triangles represent locations having USGS monitoring stations. These locations were utilized to derive bankfull channel width via satellite imagery.

2.2.SWAT

The SWAT hydrological model was used in the current study to investigate the effects of channel geometry representation on basin-wide hydrology and water quality. SWAT is one of the most widely used hydrological models and a well-established tool capable of simulating various water fluxes (e.g., surface runoff, lateral flow, groundwater contribution) and plant growth. Additional model components include weather, transport of sediment, nutrients, bacteria, pesticides, and land management. SWAT is a watershed-scale, semi-distributed, continuous-time, open-source model developed by the United States Department of Agriculture (USDA) Agricultural Research Service (ARS). The model discretizes a watershed into subwatersheds, which are further discretized into unique combinations of land use, soils, and slope called hydrological response units (HRU's) (Neitsch et al., 2011).

In SWAT, the water balance calculation for each HRU considers five storages: snow, canopy storage, the soil profile with up to ten layers, a shallow aquifer, and a deep aquifer. The water balance is calculated using the following:

$$\Delta S = \sum_{t=1}^{t} (P - Q_{total} - ET - w_{seep}) \quad (1)$$

where, ΔS is the change in water storage in the soil profile, P, Q_{total}, ET, and w_{seep} are the daily amount of precipitation, total water yield, evapotranspiration, and the total amount of water exiting the bottom of the soil profile on a given day, respectively. The value of w_{seep} is a sum of the amount of water percolating out of the lowest soil layer and the amount of water flowing past the lowest boundary of the soil profile due to bypass flow. The total water yield (Q_{total}) represents an aggregated sum of surface runoff, lateral flow, and the base flow contribution to streamflow. In this research, surface runoff is computed using the NRCS-CN method based on daily rainfall observations, and the Penman-Monteith (Monteith, 1965) method is selected for estimating evapotranspiration. The Muskingum method (Cunge, 1969) is used to route runoff volume from the subbasins to the main channel.

The SWAT 2012, release 664, was used in the current study. To accurately predict stream temperature, we used the physically based equilibrium model developed by Du et al. (2018), which considers the effects of streamflow rather than only meteorological variables to simulate water temperature. The model was recompiled in the SWAT 664 FORTRAN code.

2.3. Channel geometry representation in SWAT

One of the key components of SWAT is the representation of channels, including bankfull channel width and depth. In SWAT, runoff volume from the land to the channel is calculated using either the NRCS-CN (Natural Resources Conservation Services Curve Number) or the Green-Ampt method (Neitsch et al., 2011), whereas the streamflow rate and velocity are calculated based on channel geometry parameters like cross-sectional area and hydraulic radius, which depend on bankfull width and depths. In SWAT, streamflow rate and velocity are used to route runoff, sediment, and nutrients in the channels. SWAT allows the user to input different bankfull widths and depths for specific channels, which can help improve the accuracy of the model in cases where site-specific data exists. Additionally, the model includes options to adjust channel routing parameters, which can also help to account for variability in channel geometry and improve the accuracy of hydrologic simulations.

SWAT assumes a trapezoidal shape for all channels and a 2:1 run to rise ratio (i.e., slope of 0.5) for channel sides (Neitsch et al., 2011). Bankfull (top) channel width and depth are predefined by ArcSWAT using power-regression equations borrowed from the U.S. Environmental Protection

Agency (EPA) BASINS watershed analysis system, based on the methodology of Muttiah et al. (2007), Leopold and Maddock Jr. (1953), and Allen et al. (1994):

$$W_{bank} = 1.29A^{0.6} \quad (1)$$

where W_{bank} is the bankfull channel width (m), and A is the upstream drainage area (km^2).

and

$$d_{bank} = 0.13A^{0.4} \quad (2)$$

where d_{bank} is the bankfull channel depth (m).

The bottom width of the channel is calculated from the bankfull width, bankfull depth and the inverse of the slope (z), according to equation 3:

$$W_{bottom} = W_{bank} - 2zd_{bank} \quad (3)$$

where W_{bottom} is the bottom width of the channel (m).

The cross-sectional area of flow is calculated internally as a function of flow volume and the length of the main channel. The depth of water in the channel at a given time, under no bankfull conditions, is calculated from equation 4:

$$A_{ch}(h) = \left(W_{bottom} + zh\right)h \quad (4)$$

where A_{ch} is the cross-sectional area (m^2) through which water flows in the channel, and h is the depth of water in the channel (m).

The width of the channel at water level h is calculated as:

$$W(h) = W_{bottom} + 2zh \quad (5)$$

where W is the width of the channel at water level h (m).

The volume of water held in the channel is calculated as a function of the channel length (L_{ch}) (km) and the cross-sectional area:

$$V(h) = 1000L_{ch}A_{ch}(h) \quad (6)$$

where V is the volume of water stored in the channel (m^3). When this volume of water exceeds the maximum amount that can be held in the channel, the excess water flows through the floodplain areas. The bottom width of the flood plain is assumed to be 5 times that of the bankfull width of the channel.

Flow rate and velocity computations in SWAT are tightly linked to the channel width representation and are determined as follows:

$$q = \frac{A_{ch} R^{2/3} slp^{1/2}}{n} \quad (7)$$

$$v = \frac{R^{2/3} slp^{1/2}}{n} \quad (8)$$

where q is the rate of flow in the channel (m^3/s), R is the hydraulic radius (m) calculated from A_{ch} and wetted perimeter, slp is the slope along the channel (m/m), n is Manning's coefficient for the channel, and v is the flow velocity (m/s).

SWAT uses a power-regression model to determine the amount of sediment transported by streamflow in the channel (Her et al., 2017). The maximum amount of sediment that can be transported is a function of average streamflow and peak flow and velocity, which are directly affected by channel widths.

Additionally, the equilibrium temperature approach utilized here to simulate stream temperature considers changes in streamflow and water depth and is affected by channel dimensions. The initial stream temperature is determined as a function of the streamflow discharged at the outlet of the subbasin and the total water yield contribution within the subbasin:

$$T_w = \frac{T_{w,upstream}\left(Q_{out} - sub_{wyld}\right) + T_{w,local} sub_{wyld}}{Q_{out}} \quad (9)$$

where T_w is the initial stream temperature at a given subbasin (°C), $T_{w,upstream}$ is the water temperature of the upstream subbasin (°C), Q_{out} is the streamflow at the subbasin's outlet (m^3/s), and sub_{wyld} is the total water yield generated within the subbasin (m^3/s). After T_w is calculated, the final stream temperature is determined by considering the heat exchange between water-air and water-sediment interfaces and the water travel time. For a detailed account of the stream temperature calculation process, the reader is referred to Du et al. (2018).

Water quality modeling in SWAT is in turn impacted by stream temperature since chemical reaction rates and oxygen saturation concentration are calculated based on the simulated daily water temperature:

$$k(T) = k_{20} \theta^{T_W - 20} \quad (10)$$

where $k(T)$ is the reaction rate at local temperature (d^{-1}), k_{20} is the reaction rate at 20 °C, (d^{-1}), θ is the temperature correction coefficient, and T_W is the water temperature predicted by SWAT (°C).

Thus, channel geometry representation influences not only hydrology in SWAT but also water quality modeling.

2.4. SWAT setup and input data

As a semi-distributed watershed-scale hydrological model, SWAT requires several geospatial inputs and weather forcings to simulate physical processes within a watershed. The ArcSWAT 2012 (version 10.4.19) interface was used in this research to delineate the ACT watershed and create the HRU's. First, the watershed boundary was delineated based on a 10 meters resolution digital elevation model (DEM) from the National Elevation Dataset (NED) and hydrography network from the National Hydrography Dataset (NHD). Soil map and soil characteristics (e.g., soil depth, soil hydraulic conductivity, available water capacity) needed to parameterize SWAT's soil database were obtained from STATSGO as gridded data covering the basin's drainage area. The 2016 NLCD was ingested in ArcSWAT to characterize the basin's land-use/cover distribution. As weather forcings, this research used daily precipitation, minimum/maximum temperature, relative humidity, wind speed, and solar radiation from the GridMet daily gridded dataset (Abatzoglou, 2013). Climate data at 4 km resolution from 1979 to 2020 were extracted using the centroid of each subwatershed as a spatial reference. According to Atkins et al. (2004), atmospheric deposition is an important nonpoint source across the Mobile River Basin and accounts for about 30 and 20% of the total nitrogen and phosphorous in the basin, respectively. Thus, dry and wet atmospheric deposition data were obtained from the National Atmospheric Deposition Program for stations AL03, AL10, AL19, and AL99, which fall within the domains of ACT river basin, and incorporated as input data in the models. Point source discharges from wastewater treatment plants contribute around 5% of the total nitrogen and phosphorus to the basin (Atkins et al., 2004), and thus discharge information from 90 major facilities spread across the basin were downloaded from EPA's ECHO (Enforcement and Compliance History Online) portal and added as point sources to the model.

Actual evapotranspiration (ET) was manually calibrated against remote-sensing data from MODIS (Moderate Resolution Imaging Spectroradiometer) MOD16A2 (Mu et al., 2013) algorithm in the period 2002-2020. In the southeast United States, ET from forested ecosystems can be as high as 90% of the incoming rainfall and thus consists of a key water budget component (McLaughlin et al., 2013). To accurately capture ET in the model, we derived watershed averaged MODIS ET data at the 500-m spatial and 8-day temporal resolution from Google Earth Engine (GEE) (Gorelick et al., 2017). The data was aggregated to monthly time-step and model simulations were compared to MODIS values until a reasonable agreement was found. ET sensitive parameters were borrowed from Haas et al. (2021). Similarly, to realistically capture vegetation dynamics in the model, we used the parameter values controlling the leaf area index (LAI) of evergreen forests outlined in Haas et al. (2021). The aboveground biomass of forests was adjusted based on gridded estimates from the United States Department of Agriculture (USDA) Forest Service, as described in Blackard et al. (2008). Water temperature was manually calibrated by adjusting the parameters described in Du et al. (2018). More especially, the parameters *wtmp_add*, *sub_lag*, *sub_mkt*, *sub_lambda*, and *gwtmp_sub* had calibrated values of 2, 87 (days), 1.1, 0.99, and 16 ◦C, respectively.

The complete dataset used for constructing the SWAT model for the ACT river basin, as well as their sources, are summarized in Table 1. Based on the described data, SWAT2012 (revision 664) through the ArcSWAT interface with a 10%-10%-0% (land-use, soils, slope) threshold generated 320 subbasins and 4758 HRU's. The model was run at the daily time-step from 1979 to 2020, using 3 years (1979-1981) of initialization as model warm-up period.

Table 1 - Description of the input data utilized to construct the watershed model and evaluate the model performance in simulating streamflow and stream temperature.

	Data	**Description**	**Source**

Model input data	Topography	National Elevation Dataset at 10 meters resolution	United States Department of Agriculture (USDA) Geospatial Data Gateway (https://datagateway.nrcs.usda.gov/)
	Land use	2016 NLCD	United States Department of Agriculture (USDA) Geospatial Data Gateway (https://datagateway.nrcs.usda.gov/)
	Soil	State Soil Geographic (STATSGO)	United States Department of Agriculture (USDA) Geospatial Data Gateway (https://datagateway.nrcs.usda.gov/)
	Climate	Daily precipitation, maximum/minimum temperature, solar radiation, and wind speed from 1979 to 2020	GridMet (https://www.climatologylab.org/gridmet.html)
	Atmospheric deposition	Average annual wet and dry deposition of nitrate and ammonia from 1982 to 2020	National Atmospheric Deposition Program (NADP) (http://nadp.slh.wisc.edu/)
	Point sources	Monthly discharge and loading from wastewater treatment plants from 2007 to 2020	EPA's ECHO Portal (https://echo.epa.gov/trends/loading-tool/get-data/monitoring-data-download)
Model evaluation	Water quality	Water temperature	Water Quality Portal (https://www.waterqualitydata.us/)
	Streamflow	Daily discharge from USGS gage stations shown in Figure 1	USGS Water data (https://waterdata.usgs.gov/nwis)

2.5.Alternative sources of channel width data

In SWAT, the user can modify the bankfull width and depth of main channels and tributaries in the *.rte* and *.sub* files, respectively. This study leverages different sources of channel width data and compares them against the default values assigned by ArcSWAT. Additionally, we derived measured channel width data for six rivers across the ACT river basin using the *Data Retrieval* package (De Cicco et al., 2018) in the statistical software RStudio. The monitoring stations having channel width measurements are shown in Table 2. The alternative data sources were derived from satellite imagery, a new power-regression model, a recently published global channel width database, a previously developed power-regression model (not published) for the Alabama Coastal Plain region, and LiDAR data. The data sources are explained next.

2.5.1. Channel width data from satellite imagery

This study used Streamstats (https://streamstats.usgs.gov/ss/), a web-based application developed by the United States Geological Survey (USGS), to derive bankfull channel widths at eighty-two sub-basins across the ACT river basin. The criteria utilized to select the locations where channel widths were retrieved was the presence of USGS monitoring stations (Figure 1). We opted for this approach, rather than deriving channel widths for all channels in the model, to avoid small creeks and rivers that might be difficult to measure via satellite imagery. However, measuring channel width at one location may not accurately reflect variations along the channel segment and the average width. To quantity this uncertainty, we derived channel widths with Streamstats for 30 points over a 5 km length downstream of the USGS monitoring station 02428400 (Table 2) on the Alabama river. This location was selected because it is the most downstream monitoring station and the largest river in our watershed system. Channel width was retrieved every 150 meters between the USGS monitoring station and the outlet of the subbasin in which it is located. The average channel width was 257 meters and the standard deviation 19 meters. In Streamstats, we used satellite imagery with 15 meters resolution as a base layer and the *Elevation Profile Tool* to measure channel width and generate elevation profiles at each location. Figure 2 illustrates this process.

Streamstats provides users with access to a wide range of geospatial data related to streamflow and water quality across the United States. The platform allows users to generate reports, maps, and graphs of various streamflow statistics and other hydrological data, including flow duration curves, flood frequency estimates, and basin characteristics. Streamstats is a valuable resource for hydrologists, engineers, planners, and others involved in water resources management and planning and may be leveraged for watershed modeling applications.

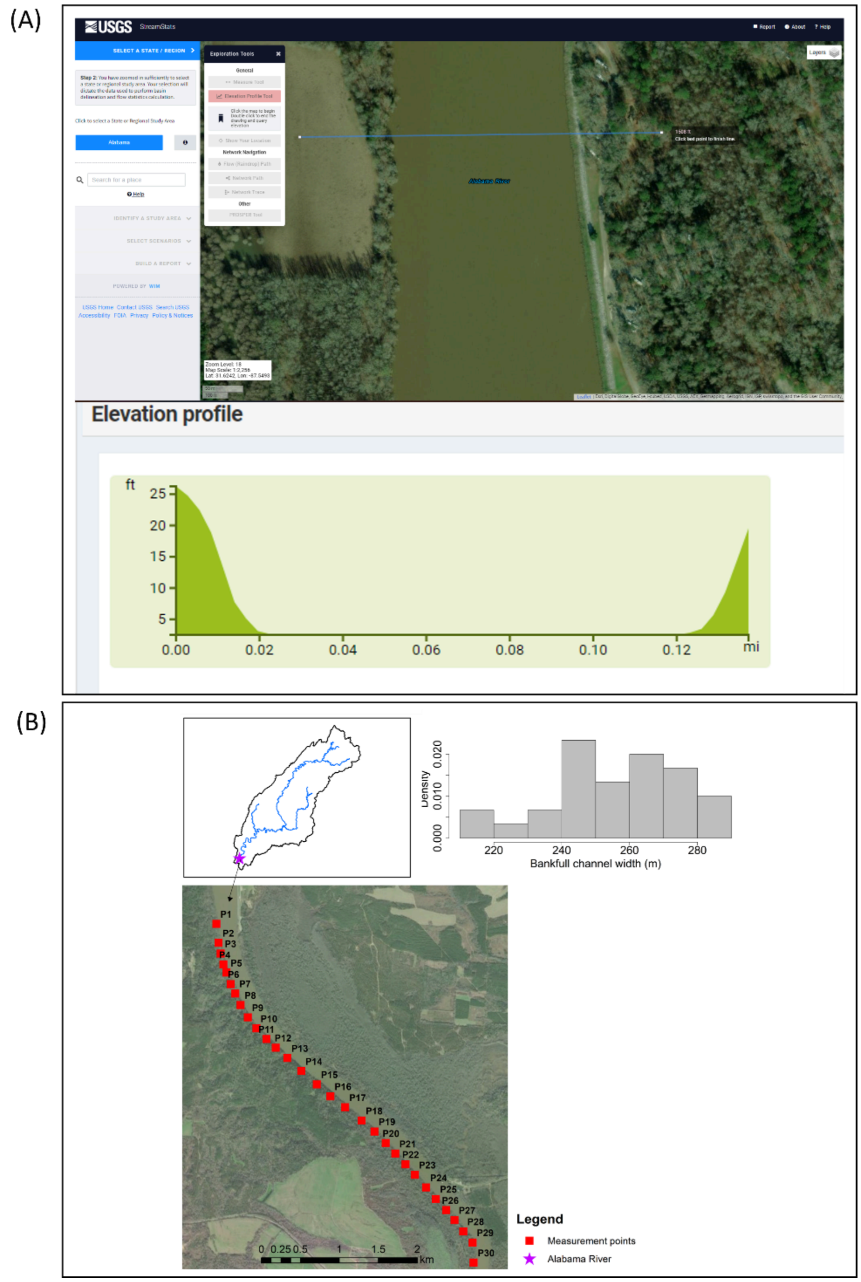

Figure 2 – (A) Screenshot of the Elevation Profile Tool in Streamstats illustrating how bankfull channel widths were retrieved (Source: Esri, DigitalGlobe, GeoEye, i-cubed, USDA FSA, USGS, AEX, Getmapping, Aerogrid, IGN, IGP, swisstopo, and the GIS User Community), (B) measuring points over the Alabama River where multiple channel widths were retrieved to capture the variations along the segment. The lat/long of the measured points are as follows: P1 (31.6055,-87.5516), P2 (31.6033,-87.5512), P3 (31.6021,-87.5508), P4 (31.6008,-87.5503), P5 (31.5999,-87.5498), P6 (31.5986,-87.5492), P7 (31.5976,-87.5485,) P8 (31.5963,-87.5477), P9 (31.5949,-87.5466), P10 (31.5937,-87.5454), P11 (31.5926,-87.5439), P12 (31.5916,-87.5426), P13 (31.5905,-87.541), P14 (31.5891,-87.539), P15 (31.5877,-87.5368), P16 (31.5864,-87.5349), P17 (31.5852,-87.5328), P18 (31.5838,-87.5305), P19 (31.5827,-87.5287), P20 (31.5814,-87.5271), P21 (31.5803,-87.5257), P22 (31.5791,-87.5242), P23 (31.578,-87.5229), P24 (31.5766,-87.5213), P25 (31.5753,-87.5199), P26 (31.5741,-87.5184), P27 (31.573,-87.5172), P28 (31.5718,-87.5159), P29 (31.5706,-87.5146), P30 (31.5682,-87.5143).

2.5.2. Development of a new power-regression model for estimating channel width

Based on the channel widths measured with Streamstats and the respective upstream sub-basin drainage areas defined in ArcSWAT, we developed a new power-regression model to estimate channel widths (Figure 3). The model is shown below and has a R^2 of 0.71.

$$W_{Streamstats} = 1.71.A^{0.485} \quad (9)$$

where $W_{Streamstats}$ is the channel width estimated by the new model (m), and A is the upstream drainage area (km^2).

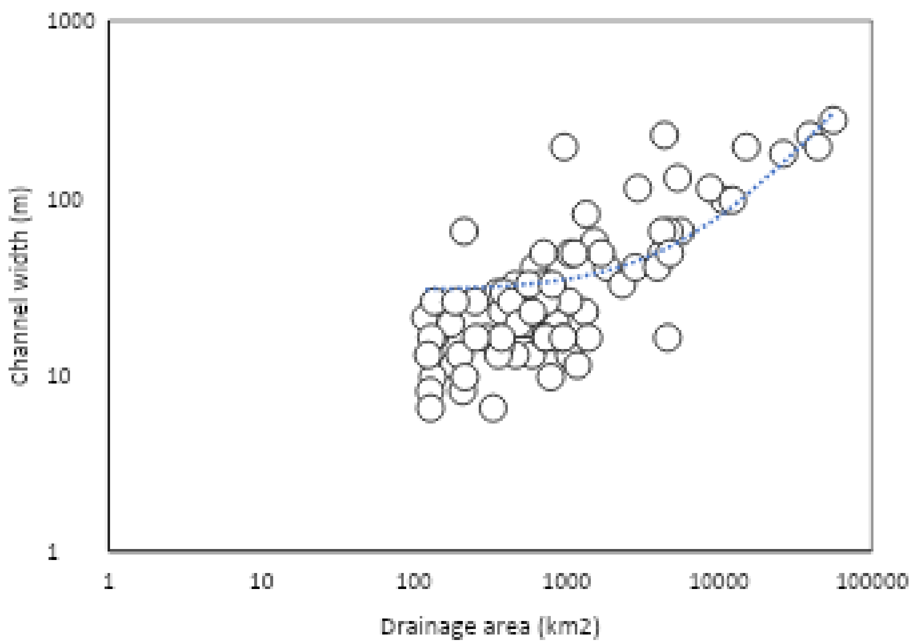

Figure 3 – The newly developed power-regression model for the ACT river basin based on Streamstats measurements.

2.5.3. Channel width from a global database

The Global River Widths from Landsat (GRWL) Database (Allen and Pavelsky, 2018) is a dataset that provides information on the widths of rivers and their associated floodplains worldwide. The data is derived from satellite imagery captured by the Landsat series of satellites. The GRWL dataset provides valuable information on the spatial distribution of river widths and the dataset is publicly available in vector format. However, channel width estimates from GRWL are yet to be tested in watershed modeling studies. The GRWL Database has over 58 million measurements of rivers wider than 30 m and the total measured area is 468,000 km^2, or 0.35% of Earth's non glaciated land surface. The GRWL's approximate spatial resolution is 30 m and the dataset is most accurate at width wider than 90 m (Allen and Pavelsky, 2018). For more details about the GRWL, the reader is referred to Allen and Pavelsky (2018).

In this study, we overlayed the GRWL vector data with the boundary and stream network of the ACT river basin produced by ArcSWAT. Next, we clipped the GRWL data to the watershed boundary using ArcMap 10.4.1 and extracted average channel width for all ACT channels contemplated in the dataset, which resulted in 31 data points. This process is illustrated in Figure 4.

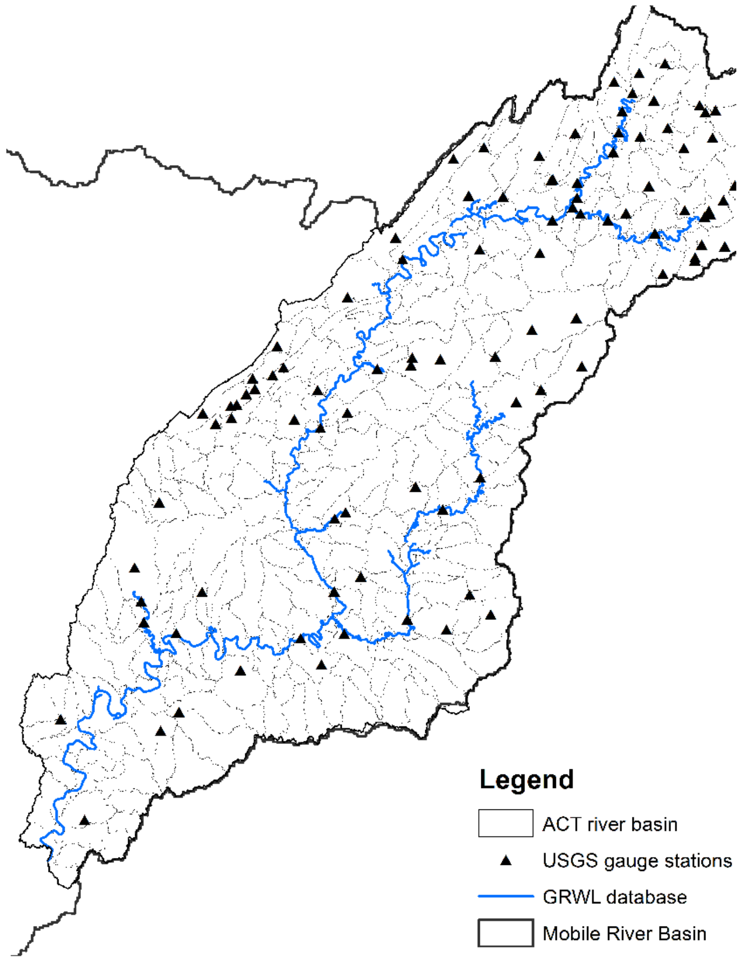

Figure 4 – Locations across the ACT river basin where bankfull channel width values from the GRWL database were extracted. Locations where USGS gauge stations overlapped with the GRWL vector were selected.

2.5.4. Channel width from a regional curve of the Alabama Coastal Plain

A study conducted by the U.S. Fish and Wildlife Service (USFWS) for the Alabama Department of Environmental Management (ADEM), Alabama Coastal Nonpoint Pollution Control Program, developed regional curves describing the relationship of dependent variables such as channel width and depth as functions of independent variables like upstream drainage area and discharge. This study was carried out in the hydro-physiographic region of the Alabama Coastal Plain and has not been published. The technical report has been shared with us via personal communication.

The relationship between bankfull channel width and drainage area has been approximated as a power function regression equation based on measurements at eight reach sites. The model, which has a R^2 of 0.94, is shown next:

$$W_{USFWS} = 5.67.A^{0.52} \qquad (10)$$

where W_{USFWS} is the bankfull channel width (ft), and A is the drainage area (mi^2).

2.5.5. Channel width from LiDAR

LiDAR (Light Detection and Ranging) technology provides an effective tool for understanding and managing stream channels by providing detailed information on their geometry and physical characteristics (Bizzi et al., 2019). LiDAR can capture highly detailed and accurate elevation data, which can be used to create digital elevation models (DEMs) and hydrologic models of channel systems (McKean et al., 2009; Passalacqua et al., 2010). With LiDAR, channel geometry parameters such as channel width, depth, cross-sectional area, and slope can be determined at fine spatial resolutions. In this study,1-meters resolution LiDAR data was used to derive bankfull channel width. LiDAR data was downloaded from the United States Geological Survey (USGS) national map viewer (https://apps.nationalmap.gov/viewer/) in LAZ format. Next, the LAZ files were converted to GeoTIFF raster format in ArcGIS Pro. Elevation from the LiDAR was used to create the output raster files and the *Natural Neighbor Triangulation* (Ferreira et al., 2010) method was employed to determine the cell values of the output raster files. Finally, the GeoTIFF files were processed using the HEC-RAS Mapper software in HEC-RAS 6.3.1. (US Army Corps of Engineers, 2023) to create terrain models from which bankfull channel widths of specific cross-sections were derived. This process is illustrated in Figure 5.

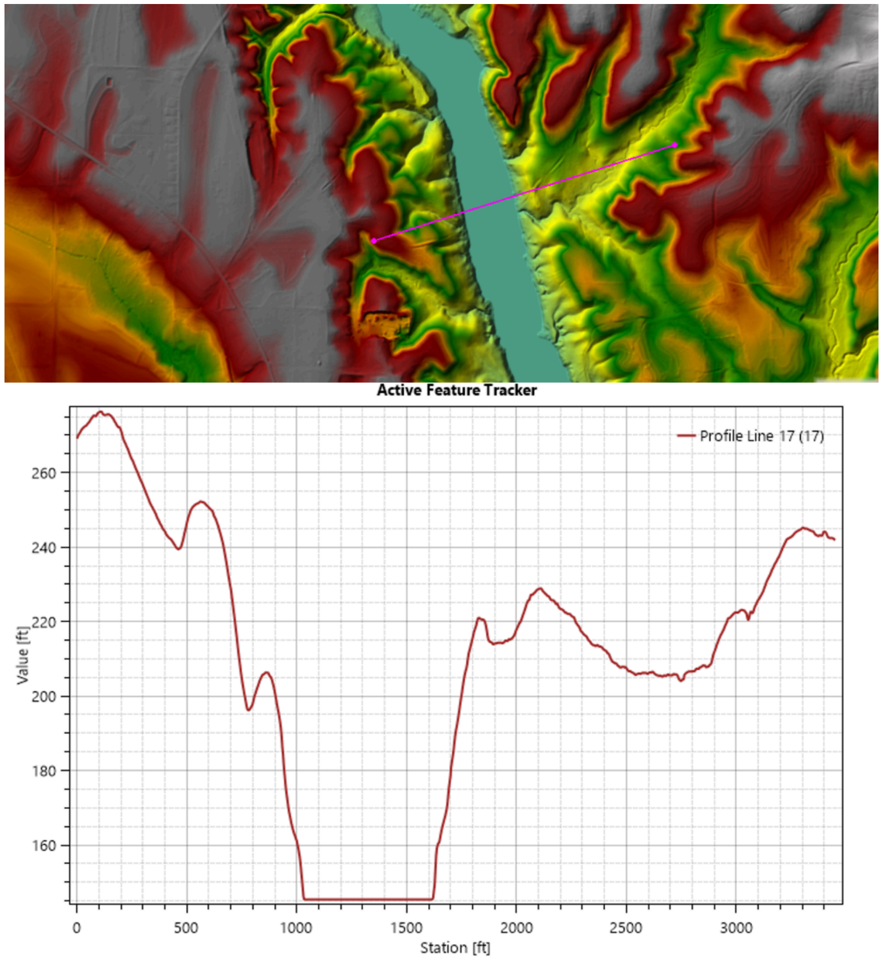

Figure 5 – Example of a terrain model created in HEC-RAS-Mapper based on LiDAR data and used to extract bankfull channel width for the USGS gauge station (02411000 COOSA RIVER AT JORDAN DAM NEAR WETUMPKA AL).

2.6.Experimental design

Modeling experiments were conducted to test the alternative sources of channel width in SWAT and assess their impacts on hydrology and stream temperature predictions across the study watershed. The modeling experiments were as follows:

1. Default SWAT (M_0): SWAT model was setup and run with the channel width values predefined by ArcSWAT;
2. Streamstats (M_{Ssts}): this scenario replaced eighty-two channel width values in the *.rte* files corresponding to the locations where channel width has been measured using Streamstats;
3. Streamstats power regression model ($M_{SstsReg}$): this scenario replaced channel width values in all three hundred twenty *.rte* files by channel widths estimated with the newly developed power-regression model explained in section 2.5.2.;
4. Global River Width Database (M_{GRWL}): this scenario replaced thirty-one channel width values in the *.rte* files by channel widths generated by the GRWL explained in section 2.5.3.;

5. Empirical model (M_{Emp}): this scenario replaced eighty-two channel width values in the *.rte* files by channel widths estimated with the regional power-regression model explained in section 2.5.4. The modified *.rte* files correspond to the locations where channel width had been previously measured using Streamstats;
6. LiDAR (M_{Lidar}): this scenario replaced thirty-one channel width values in the *.rte* files by channel widths extracted from LiDAR data. To minimize computational burden, we limited our efforts to the cross-sections where GRWL estimates were available.

Comparison of M_{Ssts} and $M_{SstsReg}$ tells us if it is feasible to develop a robust relationship between channel width and drainage area based on measurements of larger rivers in detriment of creeks and smaller channels. $M_{SstsReg}$ is an extrapolation of M_{Ssts} and meant to aid in watershed modeling studies conducted in nearby watersheds. The fourth experiment (M_{GRWL}) tells us if a global dataset having fewer data points can be a good proxy for channel width representation in watershed models. M_{Emp} tells us if regional curves may be extrapolated to nearby watersheds and be leveraged for watershed modeling applications. Finally, M_{Lidar} tells us how high-resolution LiDAR data compares against coarser and simpler estimates such as those from $M_{Ssts,}$ $M_{SstsReg,}$ $M_{GRWL,}$ and $M_{Emp.}$ M_0 serves as a reference to examine how much the default SWAT representation of channel width deviates from the alternative data sources.

2.7. Assessing the impacts of channel width on hydrology and water quality simulations

To assess the impacts of each modeling experiment on simulated daily average streamflow, 1-day maximum streamflow, and daily stream temperature, a subset of the USGS monitoring stations shown in Figure 1 was selected. We focused on USGS stations having at least 15 years of continuous time-series of streamflow data to compare model simulations against observations. Observed streamflow and water temperature data were downloaded using the *Data Retrieval* (De Cicco et al., 2018) package in the statistical software *RStudio*.

Changes in model performance from scenarios 1-6 in relation to observations of streamflow and water temperature were evaluated based on the statistical rating metrics Nash-Sutcliffe efficiency coefficient (NSE) and model percent bias (PBIAS). For detailed information about these metrics the reader is referred to Moriasi et al. (2007) and Moriasi et al. (2015).

It is worth highlighting that automated model calibration of streamflow was not carried out as our goal here is not to improve model performance, but rather investigate the impacts of channel width representation on hydrologic predictions. Additionally, semi-distributed watershed models like SWAT have hundreds of parameters controlling streamflow and adjusting them under flawed channel width representation may result in unrealistic parameter values and a model giving the right answers for the wrong reasons. Thus, to avoid the confounding effect of calibrated parameters, we followed the guidelines of Abbaspour et al. (2015) and Yen et al. (2014) to (*i*) build the model with the best datasets available prior to performing model calibration, and (*ii*) adjusted interior watershed processes (i.e.. ET, LAI, aboveground biomass) before carrying out model calibration at the watershed's outlet.

Percent changes in average streamflow, maximum flow, and stream temperature from scenarios 2-6 in relation to M_0 were examined according to equation 11:

$$Change\ in\ percent = \frac{(M_{n-}M_0)}{M_0} x100 \quad (11)$$

where M_n and M_0 are average simulations from scenarios 2-5 and M_0, respectively, over the simulation period. Table 2 summarizes the USGS stations selected for assessing the model simulations.

Table 2 – List of USGS gauge stations selected for evaluating SWAT's performance in simulating daily streamflow, maximum flow, and stream temperature using different channel width representations. The listed stations are a subset of the USGS stations shown in Figure 1.

Station ID	Station Name	Lat	Long	Drainage area (km^2)	Period of record	Variable analyzed*
02382500	COOSAWATTEE RIVER AT CARTERS, GA	34.603697	-84.69549	1349	1982-2020	Q
02388500	OOSTANAULA RIVER NEAR ROME, GA	34.298426	-85.13800	5478	1982-2020	Q
02394000	ETOWAH RIVER AT ALLATOONA DAM, ABV CARTERSVILLE, GA	34.163153	-84.74104	2906	1982-2020	Q
02395980	ETOWAH RIVER AT GA 1 LOOP, NEAR ROME, GA	34.232317	-85.11689	4665	1982-2020	Q
02397000	COOSA RIVER NEAR ROME, GA	34.200373	-85.25662	10464	1982-2020	Q, T
02398000	CHATTOOGA RIVER AT SUMMERVILLE, GA	34.466389	-85.33611	497	1982-2020	Q
02399200	LITTLE RIVER NEAR BLUE POND AL	34.28787	-85.68163	515	1982-2020	Q
02401390	BIG CANOE CREEK AT ASHVILLE AL	33.839821	-86.26275	365	1982-2020	Q
02412000	TALLAPOOSA RIVER NEAR HEFLIN, ALA.	33.622885	-85.51328	1160	1982-2020	Q, T
02414500	TALLAPOOSA RIVER AT WADLEY AL	33.116787	-85.56078	4338	1982-2020	Q
02419000	UPHAPEE CREEK NEAR TUSKEGEE AL	32.476805	-85.69495	862	1982-2020	Q
02422500	MULBERRY CREEK AT JONES AL	32.58291	-86.90359	526	1982-2020	Q
02424000	CAHABA RIVER AT CENTREVILLE AL	32.945124	-87.13916	2660	1982-2020	Q
02425000	CAHABA RIVER NEAR MARION JUNCTION AL	32.444025	-87.18027	4574	1982-2020	Q
02428400	ALABAMA RIVER AT CLAIBORNE L&D NEAR MONROEVILLE	31.6151	-87.5505	55615	1982-2020	Q, T
02401000	BIG WILLS CREEK NEAR REECE CITY	34.098152	-86.03802	1476	1986-2020	Q
02404400	CHOCCOLOCCO CREEK AT JACKSON SHOAL NR LINCOLN AL	33.548438	-86.09691	1246	1984-2020	Q
02407514	YELLOWLEAF CREEK NEAR WESTOVER, ALA	33.320667	-86.49525	368	2005-2020	Q
02411000	COOSA RIVER AT JORDAN DAM NEAR WETUMPKA AL	32.61402	-86.25497	26164	1982-2013	Q
02419890	TALLAPOOSA RIVER NEAR MONT.-MONT. WATER WORKS	32.439859	-86.19552	12033	1995-2020	Q
02420000	ALABAMA RIVER NEAR MONTGOMERY, AL	32.411526	-86.40830	39075	1982-2020	Q
02423555	CAHABA RIVER NEAR HELENA AL	33.284558	-86.88249	868	1995-2020	Q
02423496	CAHABA RIVER NEAL HOOVER AL	33.3692767	-86.78415	585	1991-2019	Q, T
21AWIC	COOSA RIVER JORDAN DAM AL	32.6140204	-86.25497	26164	2005-2020	Q, T
02787000	CONASAUGA RIVER AT TILTON GA	34.6669167	-84.92791	1836	2014-2022	W
02388520	OOSTANAULA RIVER AT ROME GA	34.2692599	-85.17273	5555	2014-2022	W
02392000	ETOWAH RIVER AT CANTON GA	34.2401944	-84.49453	1588	2014-2022	W
02394980	ETOWAH RIVER AT HARDIN BRIDGE RD GA	34.1889849	-84.92522	4175	2014-2022	W
02413210	LITTLE TALLAPOOSA R AT GA 100	33.4926944	-85.27931	634	2014-2022	W
02429500	ALABAMA RIVER AT CLAIBORNE AL	31.5468275	-87.51249	56894	2014-2022	W

* Q = Streamflow, T = Stream temperature, W = Channel width.

3. Results

3.1. Leveraging alternative data sources to capture channel width

The default representation of channel width in SWAT showed substantially larger channel width values compared to the alternative sources (Figure 6). Channel widths were compared among scenarios 1-6 at thirty-one locations where we had estimates from all sources. Average channel widths ± standard deviation from M_0, M_{Ssts}, $M_{SstsReg}$, M_{GRWL}, M_{Emp}, and M_{Lidar} were 258 ± 223 m, 90 ± 73 m, 71 ± 50 m, 82 ± 60 m, 100 ± 74 m, and 117 ± 69 m, respectively. Average channel width from the alternative sources was 92 ± 16 meters, almost three times smaller than SWAT's average value. Overall, M_{Ssts}, $M_{SstsReg}$, M_{GRWL}, M_{Emp}, and M_{Lidar} showed good agreement with each other, with $M_{SstsReg}$ and M_{Lidar} having the extreme values of 71 ± 50 m and 117 ± 69 m, respectively. The channel width estimates from M_{Ssts} and M_{GRWL} showed particularly good agreement, with an average difference of only 8 meters.

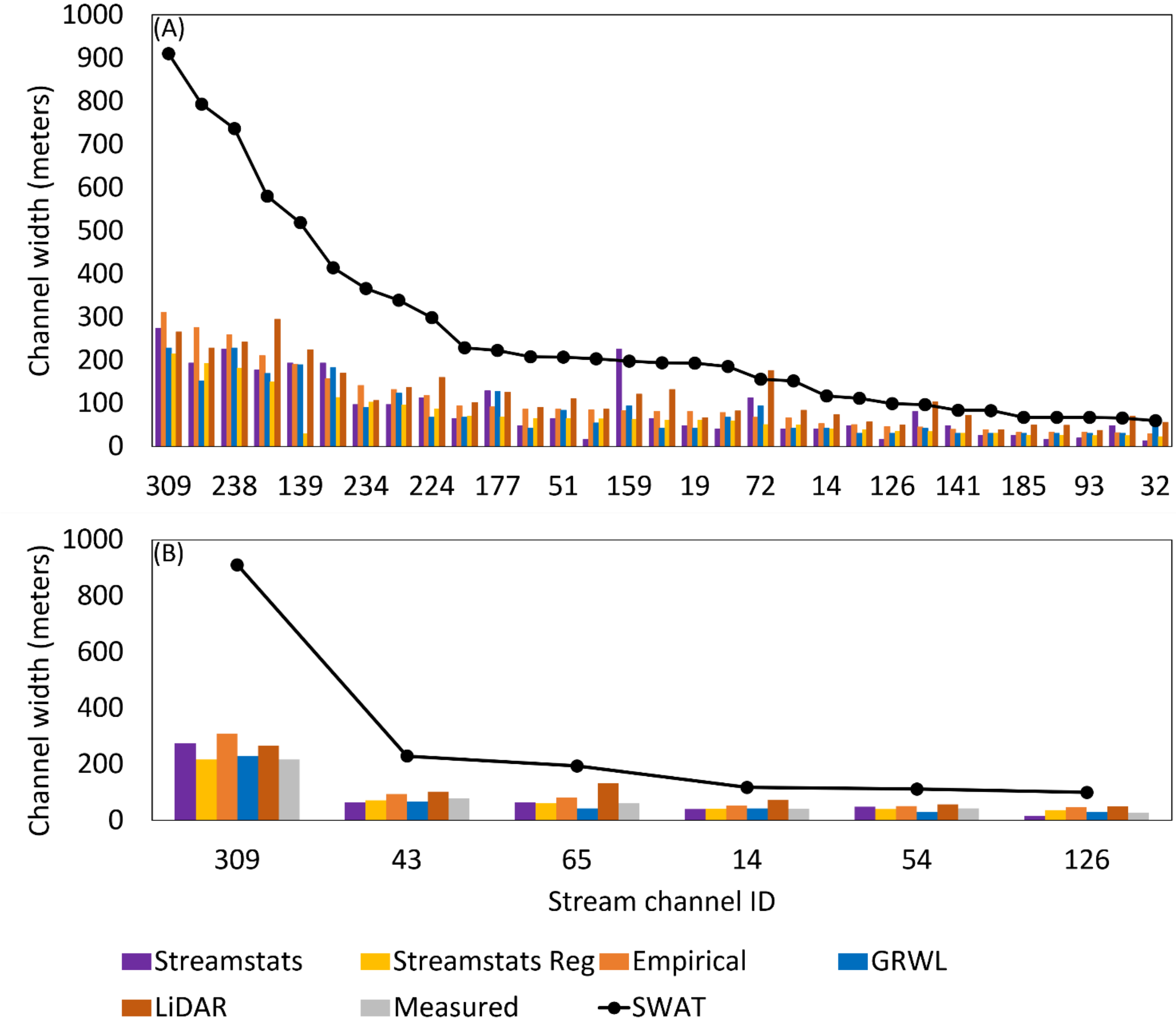

Figure 6 - Comparison of channel width values from (A) default SWAT and alternative sources, and (B) default SWAT, alternative sources, and measured data. Stream channel drainage areas decrease from left (downstream) to right (upstream).

The alternative data sources showed overall good agreement with measured channel widths for the locations where we had estimates, with NSE values ranging from 0.66 to 0.99 (Figure 6B and

Table 3). Conversely, M_0 overestimated measurements by 258% and had a negative NSE. Estimates from $M_{SstsReg}$ and M_{GRWL} had the best performance in capturing channel widths, while data from M_{Emp} and M_{Lidar} had the poorest agreements with measurements among the alternative sources.

Table 3 – Statistical performance of alternative data sources of channel width compared to measured data at six rivers across the ACT river basin.

	SWAT	Streamstats	Streamstats Reg	Empirical	GRWL	LiDAR
NSE	-17.21	0.87	0.99	0.66	0.97	0.66
PBIAS (%)	-258	-9.2	-0.3	-36.43	5.4	-46.1

3.2. Impacts of channel width representation on mean daily streamflow

The model skills in capturing daily streamflow for the periods and locations shown in Table 2 were assessed based on NSE and PBIAS values. Figure 7 shows how the model performance changed in terms of NSE under scenarios 1-6. SWAT performed well under M_0 (Figure 7a), with NSE values increasing from lower to higher stream orders (i.e., upstream to downstream locations). Negative NSE values were found at only three of the twenty-two study locations and those were small headwater channels in the upper portion of the watershed. Under scenarios 2-6, SWAT yielded similar NSE patterns, with model performances improving from lower to higher stream orders. However, all alternative sources of channel width led to deterioration in NSE compared to M_0, with negative NSE values found at five locations. Disregarding the two locations where NSE < -2, average NSE was 0.43 for M_0, whilst it dropped to 0.14 for M_{Ssts} and $M_{SstsReg}$, and 0.13 for M_{GRWL}, M_{Emp}, and M_{Lidar}. Under M_{Ssts}, $M_{SstsReg}$, M_{GRWL}, M_{Emp}, and M_{Lidar} SWAT's performance in capturing daily streamflow was very similar, with no or negligible differences, as illustrated in Figures 7b-f and in the bar plot at the bottom of Figure 7.

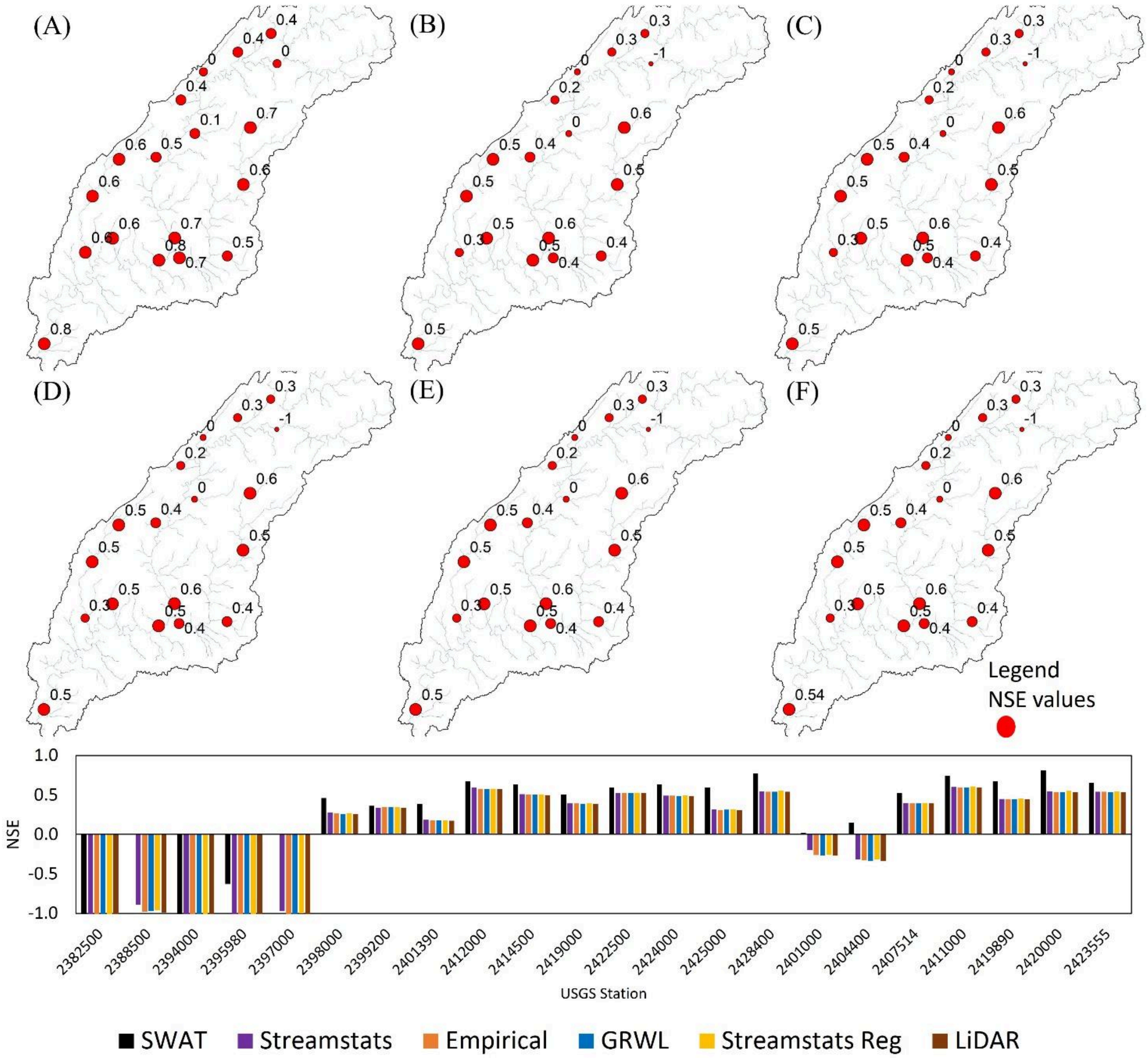

Figure 7 – Model performance in terms of the Nash Sutcliffe efficiency coefficient (NSE) in simulating daily streamflow at selected USGS stations under different channel width representations – SWAT (A), Streamstats (B), Streamstats Reg (C), Empirical (D), GRWL (E), and LiDAR (F). The size of the red circles are proportional to the NSE values, with larger circles representing the best model performances.

Similarly, Figure 8 shows how the model performance changed from scenarios 1-6 in terms of PBIAS. Positive values indicate model underestimation of streamflow, while negative values indicate model overestimation. There was virtually no change in PBIAS among all model configurations. Although slight variations in PBIAS happened because of different channel width representations at some sites, average PBIAS was -38.81% for all scenarios. Overall, SWAT largely overestimated daily streamflow across the ACT river basin, with larger PBIAS values found in the northern and northwest portions of the watershed. Above average PBIAS values were predominantly found at smaller reaches in creeks, except for the Cahaba River near Helena AL (USGS 02423555), where a 49.78% model overestimation was found. Locations having drainage areas larger than 1,000 km^2 usually witnessed model overestimation of streamflow lower than 20%.

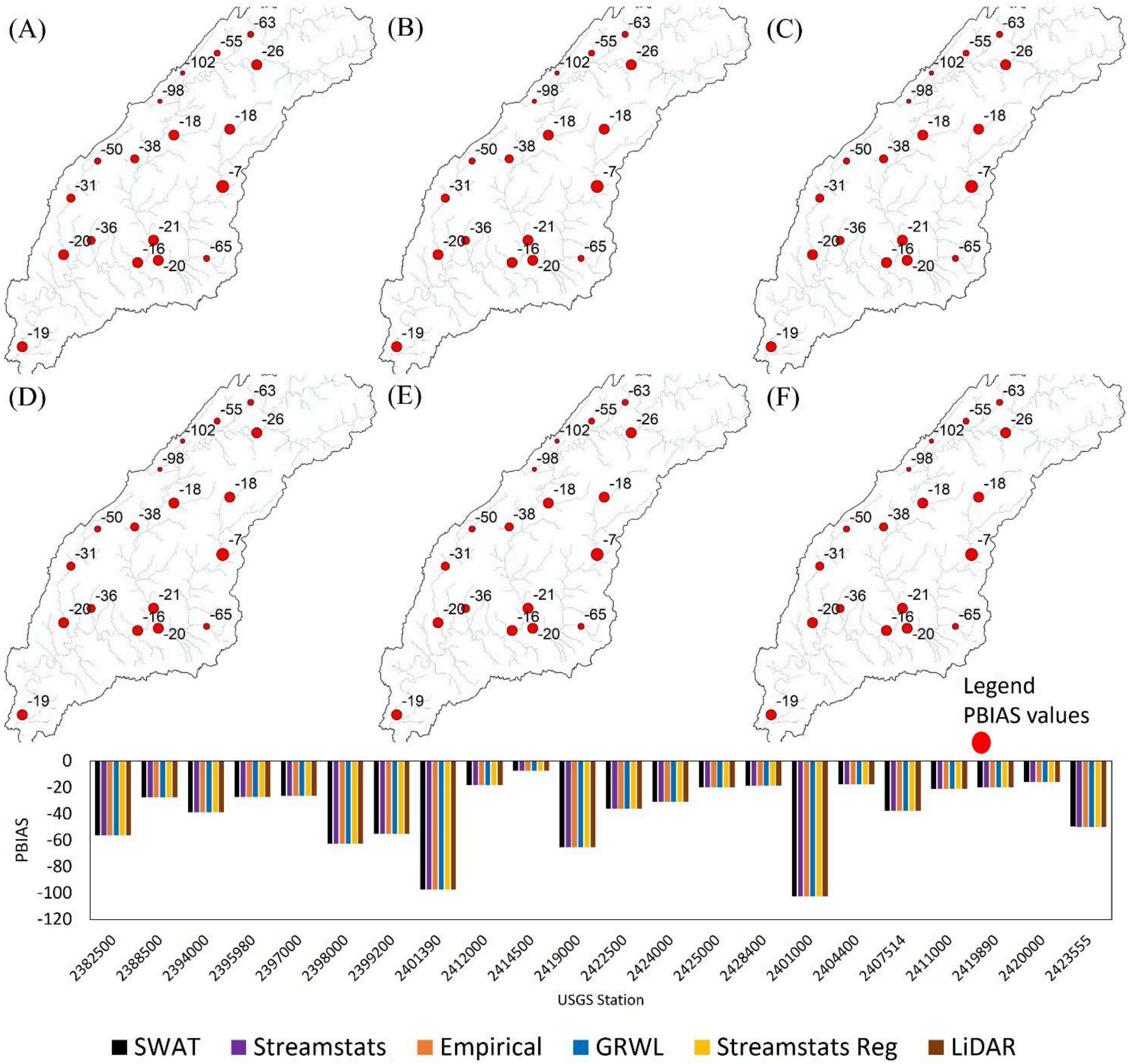

Figure 8 - Model performance in term of model percent bias (PBIAS) (%) in simulating daily streamflow at selected USGS stations under different channel width representations - SWAT (A), Streamstats (B), Streamstats Reg (C), Empirical (D), GRWL (E), and LiDAR (F). The size of the red circles is proportional to the PBIAS values, with larger circles showing the best model performances.

3.3.Impacts of channel width representation on maximum flows

Channel width representation showed substantial impacts on model simulations of 1-day maximum flow. Percent differences in simulated 1-day maximum flows in relation to observations are shown in

Figure 9 for scenarios 1-6. Positive (upward green arrows) values indicate locations where maximum flow was overestimated by the model, whereas negative (downward red arrows) values indicate model underestimation of maximum flow. Absolute percent differences were higher in lower stream orders with all model configurations, corroborating the results that model agreement with observations increases from upstream to downstream in the ACT river basin. Under M_0, SWAT underestimated maximum flow at fourteen of the twenty-two study locations. However, the average percent difference from observed data was 23% model overestimation. Model overall overestimation of 1-day maximum flow, despite showing underestimation at most sites, is a result of major overestimations at lower stream order locations. Under scenarios M_{Ssts}, $M_{SstsReg}$, M_{GRWL}, M_{Emp}, and M_{Lidar} SWAT underestimated 1-day maximum flow at only nine sites and showed average overall overestimations of 48.63, 48.99, 49.75, 49.69, and 49.99%, respectively. M_{Ssts} had the best performance among the alternative sources, although the percent difference in relation to the observations was still large.

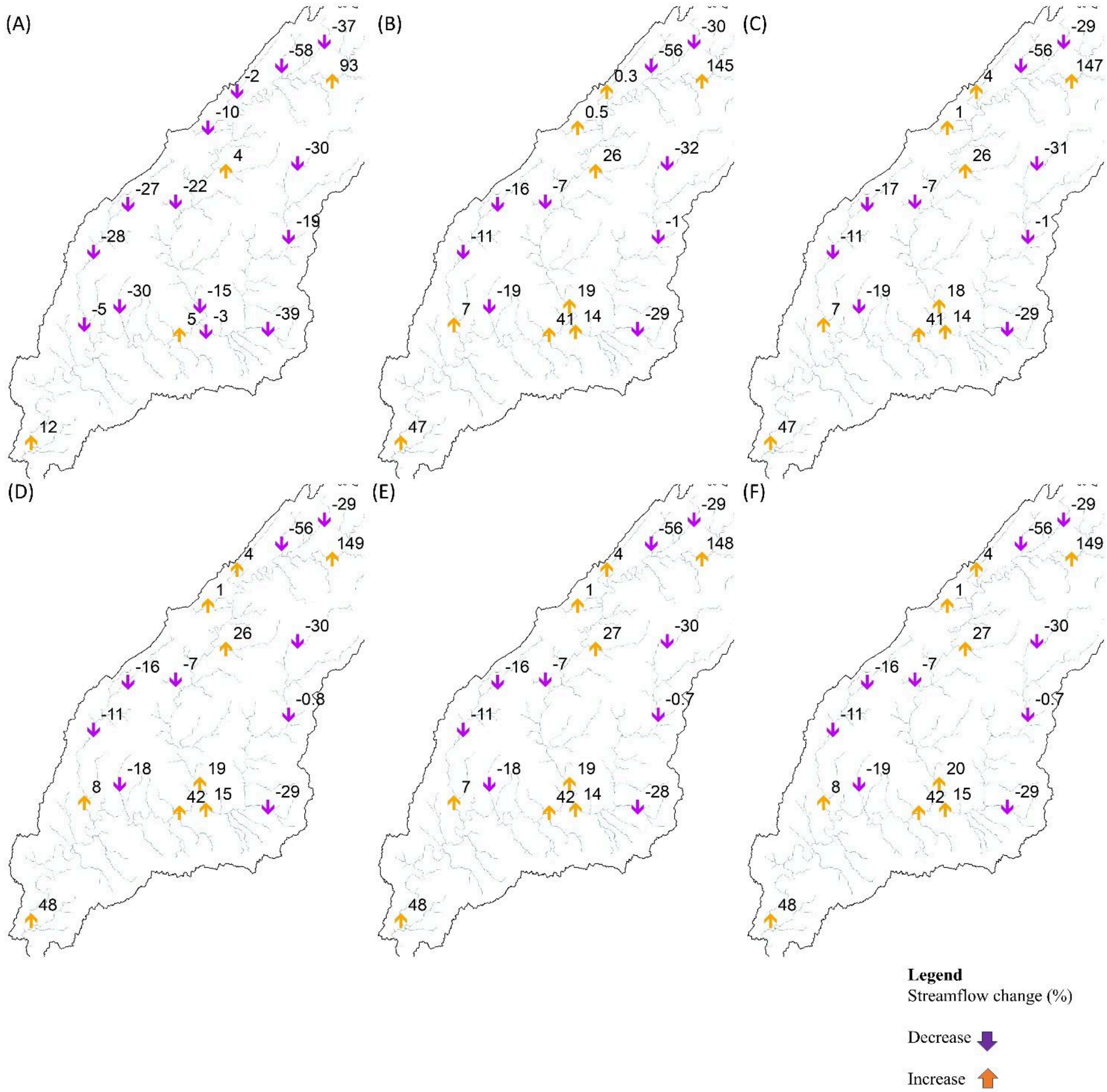

Figure 9 – Percent change in 1-day maximum flows in relation to observations under different channel width representations - SWAT (A), Streamstats (B), Streamstats Reg (C), Empirical (D), GRWL (E), and LiDAR (F).

The global effects of using alternative sources of channel width in SWAT for simulating maximum flows was that of improving the model agreement with observations at ten of the twenty-two study locations.

Although M_{Ssts}, $M_{SstsReg}$, M_{GRWL}, M_{Emp}, and M_{Lidar} yielded similar results in estimating maximum flows, there were some differences among these scenarios. Figure 10 illustrates this by showing the percent changes in simulated maximum flow between each scenario and M_0. Positive values indicate percent increases in maximum flow, while negative values indicate percent decreases. The average percent change in simulated maximum flow from scenarios 2-6 in relation to M_0 was

20.32%, with individual values of 19.79, 20.11, 20.75, 20.65, and 20.88% for M_{Ssts}, $M_{SstsReg}$, M_{GRWL}, M_{Emp}, and M_{Lidar}, respectively. Overall, M_{Ssts} had the smallest impacts in simulated maximum flow, while M_{Lidar} showed the largest impacts. This result is further illustrated in the bar plot at the bottom of Figure 10.

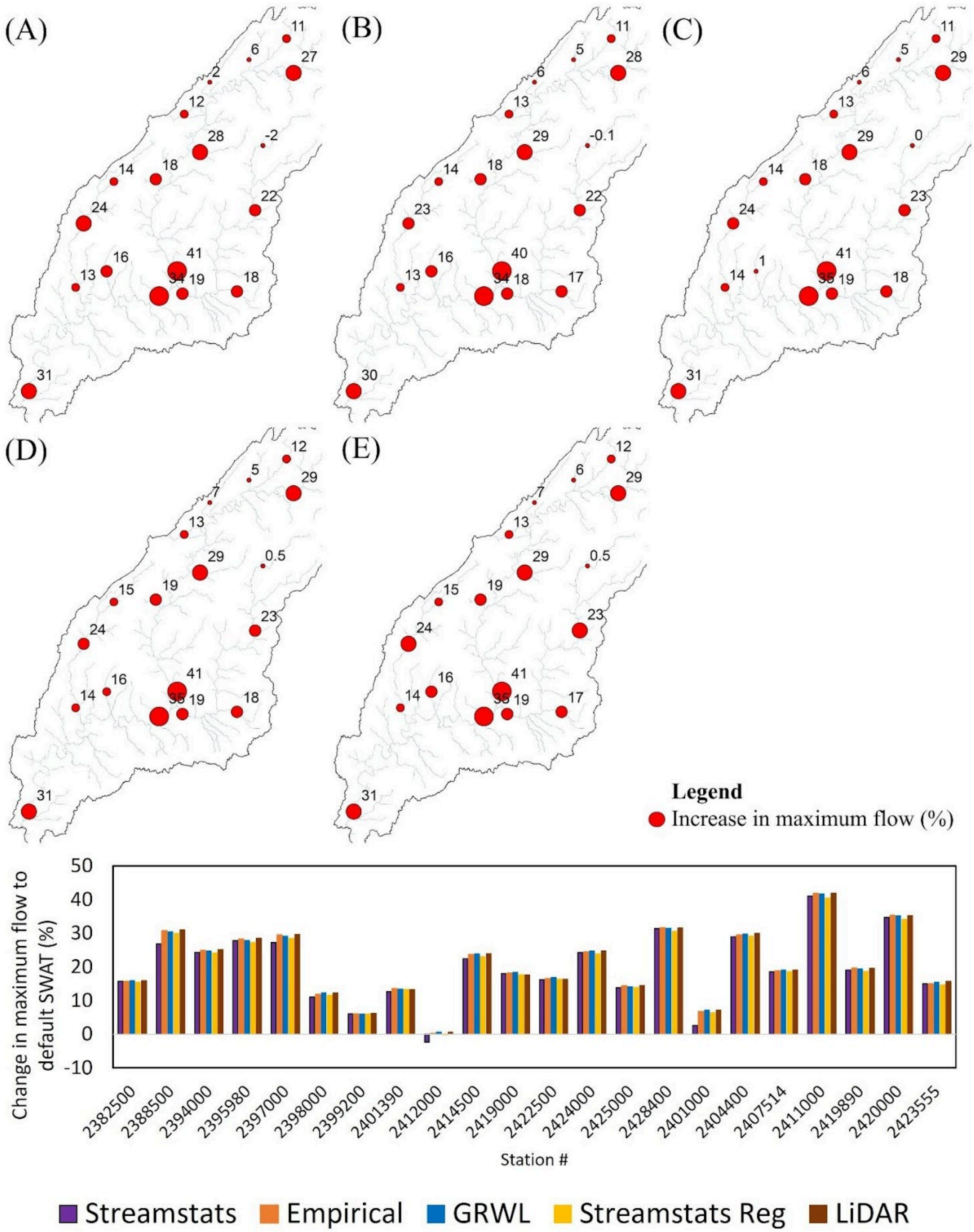

(A)
(B)
(C)
(D)
(E)
Legend
Increase in maximum flow (%)
Change in maximum flow to default SWAT (%)
50
40
30
20
10
0
-10
2382500
2388500
2394000
2395980
2397000
2398000
2399200
2401390
2412000
2414500
2419000
2422500
2424000
2425000
2428400
2401000
2404400
2407514
2411000
2419890
2420000
2423555
Station #
Streamstats
Empirical
GRWL
Streamstats Reg
LiDAR

Figure 10 – Percent change in 1-day maximum flow in relation to default SWAT under different channel width representations - Streamstats (A), Streamstats Reg (B), Empirical (C), GRWL (D), and LiDAR (E).

3.4.Impacts of channel width representation on stream temperature

Average daily stream temperatures simulated with SWAT under M_0, M_{Ssts}, $M_{SstsReg}$, M_{GRWL}, M_{Emp}, and M_{Lidar} are illustrated in Figures 11a-f, respectively. Overall, all alternative sources led to lower water temperatures compared to default SWAT. Average daily water temperatures at the study sites were 19.2, 18.7, 18.4, 18.9, 18.8, and 19.1°C with M_0, M_{Ssts}, $M_{SstsReg}$, M_{GRWL}, M_{Emp}, and M_{Lidar}, respectively. The bar plot at the bottom of Figure 11 clearly shows that M_0 predicted the highest daily average stream temperatures amongst all scenarios.

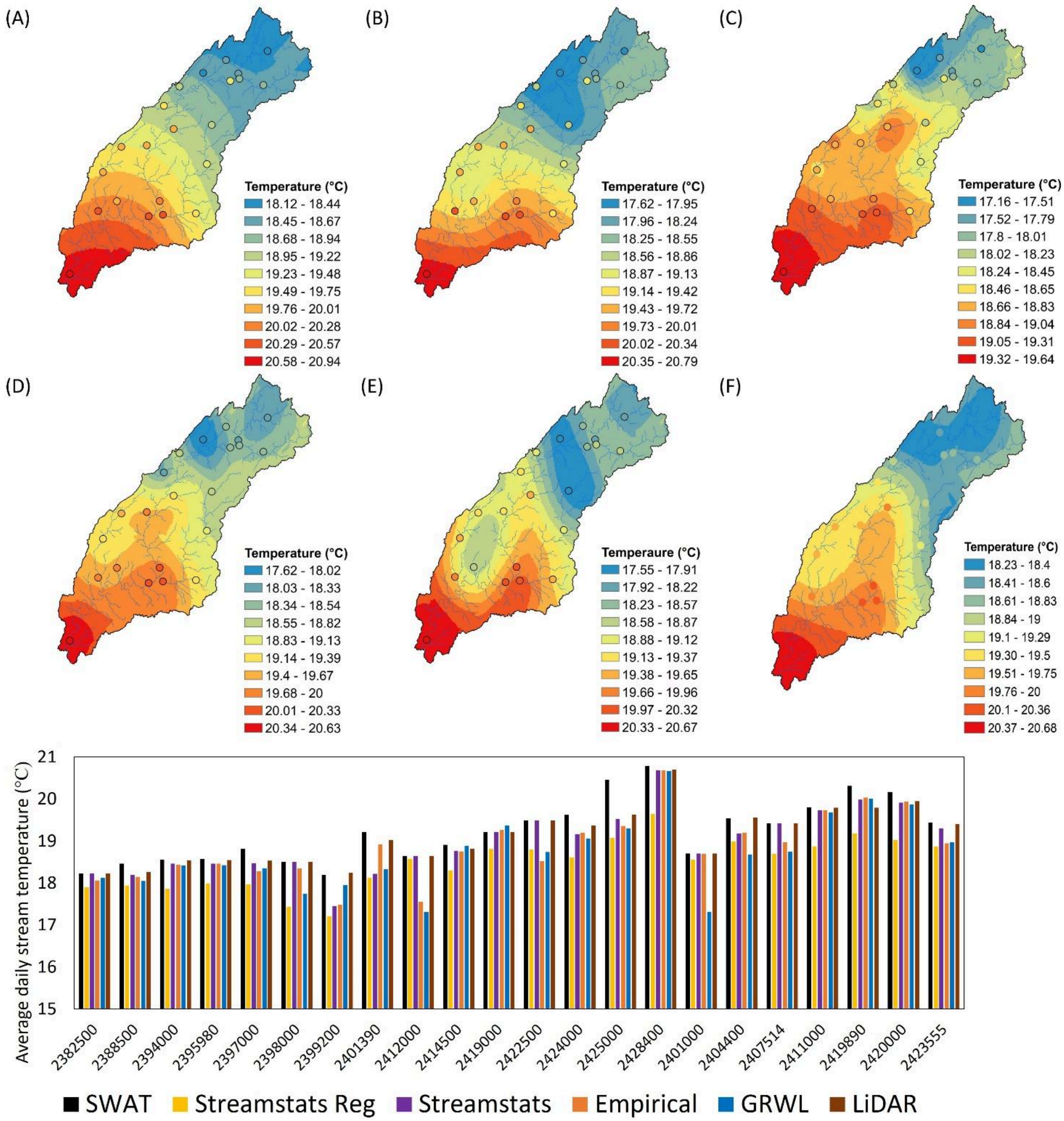

Figure 11 – Average daily stream temperature simulations under different channel width representations - SWAT (A), Streamstats (B), Streamstats Reg (C), Empirical (D), GRWL (E), and LiDAR (F).

The percent change in simulated average daily stream temperature from each scenario compared to M_0 is shown in Figure 12. Positive values indicate increases in simulated stream temperature compared to M_0, while negative values indicate decreases. Overall, M_{Ssts}, $M_{SstsReg}$, M_{GRWL}, M_{Emp}, and M_{Lidar} resonated in lower stream temperatures with an average -2% in relation to M_0. The relative changes from M_{Ssts}, $M_{SstsReg}$, M_{GRWL}, $M_{Emp,}$ and M_{Lidar} were -1.26, -3.91, -2.63, -1.91, and -0.51%, respectively.

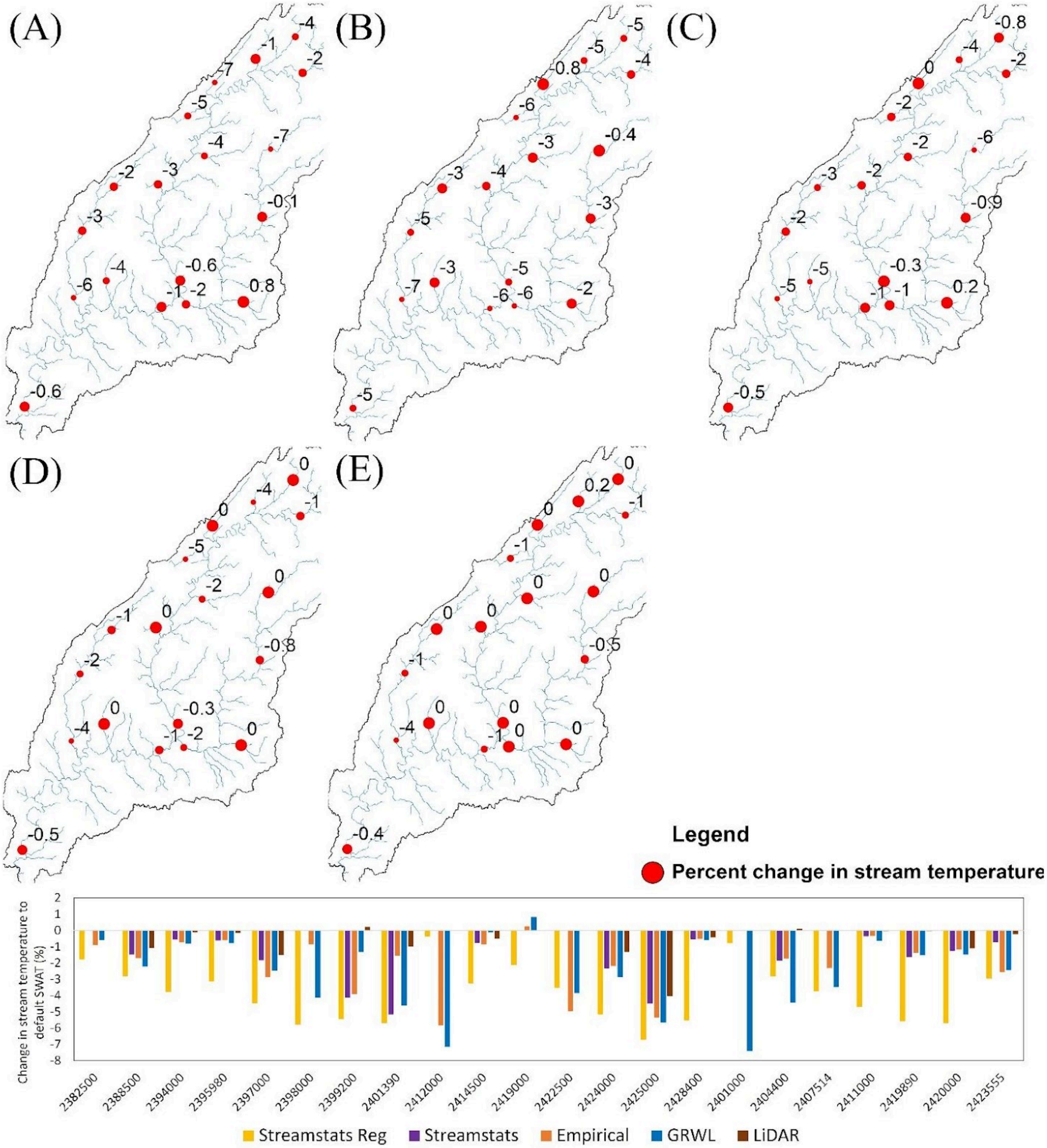

Figure 12 – Percent change in daily stream temperature simulations in relation to default SWAT under different channel width representations - Streamstats (A), Streamstats Reg (B), Empirical (C), GRWL (D), and LiDAR (E).

Model performance in simulating daily stream temperature was evaluated against observations at five locations with relatively good data record (Table 2). Daily simulations versus observations were averaged to seasonal time-step for clarity purposes and are shown in Figure 13. The alternative sources of channel width improved the model performance in terms of NSE and

PBIAS at all sites (Table 4). The statistical rating metrics summarized in Table 4 refer to daily simulations. Overall, SWAT overestimated stream temperature under all scenarios and at all sites, except at 21AWIC (Figure 13b). Average NSE values predicted with M_0, M_{Ssts}, $M_{SstsReg}$, M_{GRWL}, M_{Emp}, and M_{Lidar} were 0.61, 0.69, 0.7, 0.63, 0.72, and 0.63, respectively. In terms of PBIAS, M_0, M_{Ssts}, $M_{SstsReg}$, M_{GRWL}, M_{Emp}, and M_{Lidar} yielded -5.4, -1.3, -0.7, -4.7, -1.5, and -2,3%, respectively. On average, M_{Emp} and $M_{SstsReg}$ achieved the best performances for NSE and PBIAS, respectively. It can be seen that the differences in simulated stream temperature from the alternative sources in relation to M_0 were usually more pronounced during the spring and summer seasons.

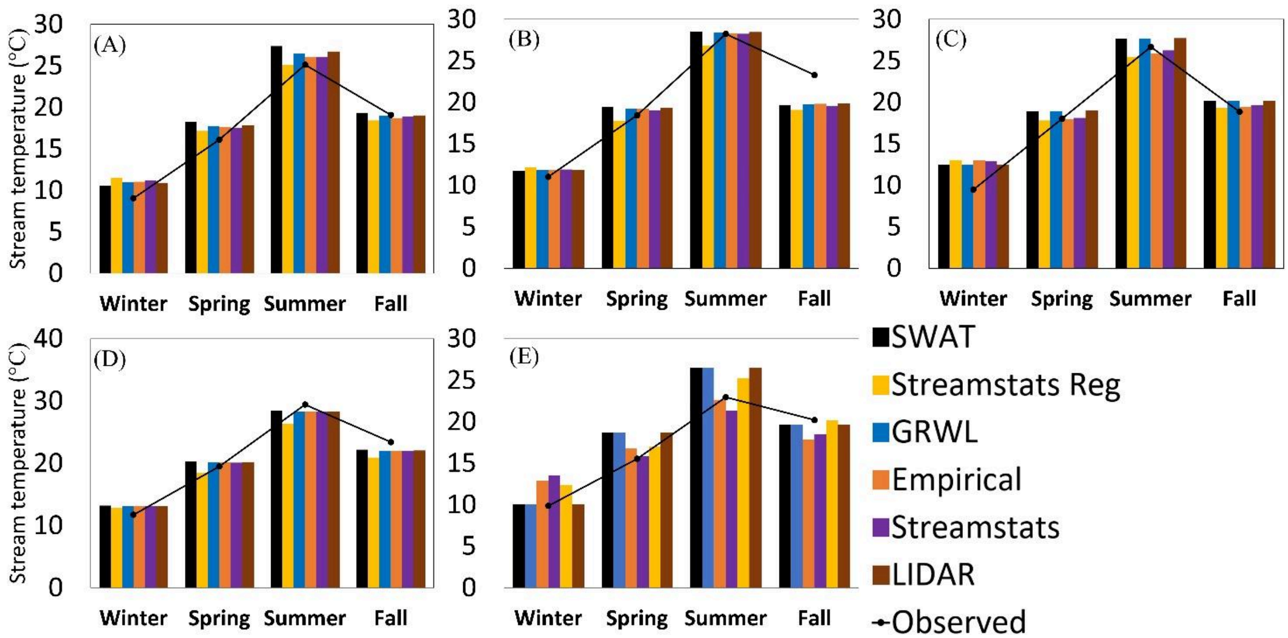

Figure 13 – Comparison of simulated versus observed daily stream temperature under different channel width representations at the sites USGS 02397000 (A), 21AWIC (B), USGS 02423496 (C), USGS 02428400(D), and USGS 02412000 (E).

Table 4 – Model performance in simulating daily streamflow temperature under different channel width representations at the rivers shown in Figure 13.

		SWAT	Streamstats Reg	GRWL	Empirical	Streamstats	LiDAR
Coosa 1	NSE	0.74	0.87	0.82	0.87	0.83	0.81
	PBIAS (%)	-8.95	-4.0	-6.9	-5.8	-6.2	-7.25
Cahaba	NSE	0.78	0.81	0.78	0.79	0.80	0.78
	PBIAS (%)	-8.51	-3.5	-8.5	-4.4	-5.4	-8.51
Alabama	NSE	0.82	0.82	0.83	0.83	0.83	0.83
	PBIAS (%)	-1.37	5.71	-0.53	-0.56	-0.40	-0.64
Tallapoosa	NSE	-0.03	0.25	-0.03	0.38	0.23	-0.03
	PBIAS (%)	-9.93	-8.0	-9.9	1.2	3.0	2.96
Coosa 2	NSE	0.72	0.73	0.74	0.75	0.73	0.74

	PBIAS (%)	1.9	6.4	2.2	2.2	2.7	1.95

3.5.Impacts of channel width representation on sediment and nutrients loadings

Sediment and nutrient loading simulations showed important sensitivity to channel width representation in SWAT (Figure 14). Total annual sediment loading predicted by M_0 was significantly higher compared to the alternative data sources (Figure 14A). Under M_{Ssts}, $M_{SstsReg}$, M_{GRWL}, M_{Emp}, and M_{Lidar}, total annual sediment loading exceeded M_0 by 114, 109, 116, 113, and 118%, respectively.

In contrast, simulated total annual nitrate loading exhibited a decrease under M_{Ssts}, $M_{SstsReg}$, M_{GRWL}, M_{Emp}, and M_{Lidar} compared to M_0 (Figure 14B), with percent changes ranging from -7.1% to -8.3%. Among these scenarios, simulations with $M_{SstsReg}$ and M_{Lidar} demonstrated the highest (-8.3%) and lowest (-7.1%) percent changes relative to M_0.

Similarly, total annual phosphate loadings simulated with the alternative data sources were consistently lower than those predicted by the default model (Figure 14C). Simulated phosphate loadings were similar under M_{Ssts}, $M_{SstsReg}$, M_{GRWL}, M_{Emp}, and M_{Lidar}, with $M_{SstsReg}$ and M_{Lidar} resulting in the highest (-18.8%) and lowest (-15.1%) percent changes compared to M_0.

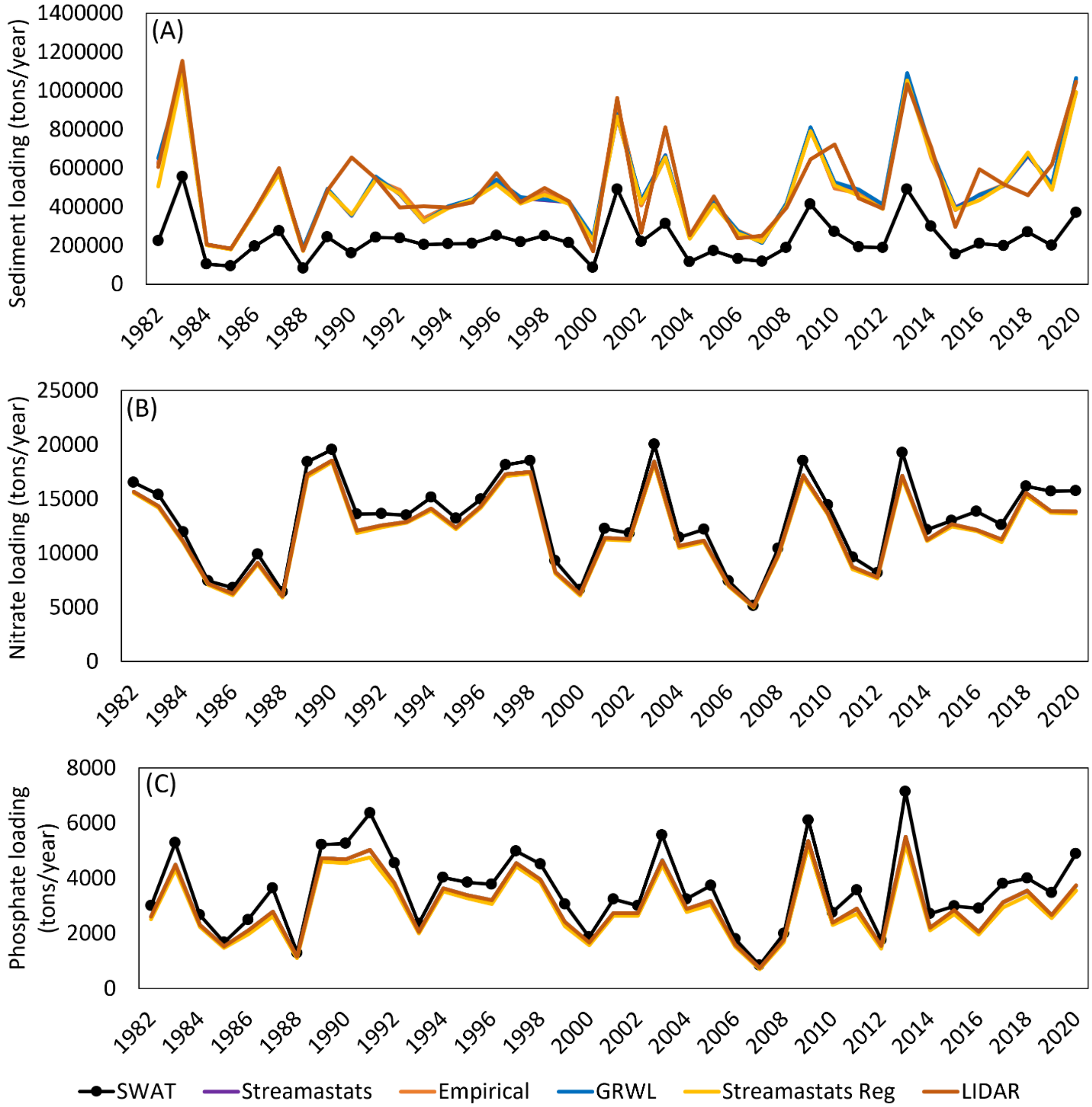

Figure 14 – Total annual sediment, nitrate, and phosphate loading simulated at the most downstream watershed outlet (USGS 02428400).

4. Discussion

Many times, watershed models are calibrated at target locations such as the watershed outlet for a single variable like streamflow. However, there are many other internal watershed processes occurring between the outlet and upland areas (e.g., evapotranspiration, soil moisture, vegetation growth) that may not be accurately simulated. In hydrologic modeling, this is commonly known as “getting the right answers for the wrong reasons”, and essentially refers to situations where a model produces accurate results, but the underlying assumptions or input data used in the model are incorrect or inappropriate. In the era of open-source earth system science data, it is time for watershed modelers to leverage the existence of alternative datasets and approaches to enhance the reliability of hydrologic models in representing watershed conditions such as bankfull width, instead of solely relying on empirical relationships. Our study is the first to address this issue at a regional level and to propose simple, yet robust, alternative approaches to enhance the representation of channel geometry in watershed models.

Our results showed that the default regression equation used in ArcSWAT to estimate bankfull width led to substantially wider channels compared to five alternative datasets derived from varying sources. This was further corroborated by comparing estimates from the alternative datasets with measured values at six rivers across the watershed system. Results showed that the default SWAT overestimated measured values by more than 200%, while the alternative datasets had overestimations ranging from 46 to 0.3%. This indicates the potential of our proposed approaches to help modelers and stakeholders to either estimate channel widths or better represent it in watershed models. Our findings reveal that without user adjustment SWAT misrepresents bankfull channel width and our findings concur with those of Her et al. (2017) and Han et al. (2019), which showed that ArcSWAT provides larger channel widths compared to field surveys and remote-sensing measurements. However, our results disagree with Kim et al. (2022), which showed that default regression equation used in ArcSWAT underestimated channel width in a small watershed in South Korea.

In the current study, impacts of channel width representation on mean daily streamflow predictions were twofold. First, model performance in terms of NSE significantly changed after replacing SWAT’s default channel width values with estimates from five alternative sources derived from satellite data, empirical models, LiDAR data, and a global dataset. Second, model over and underestimation of observed streamflow, measured with PBIAS values, was not affected by channel width representation. This finding suggests that channel width has important implications for the timing and rate of simulated streamflow, whilst it has no implications for water balance computation. Although the latter might seem obvious, channel evaporation losses in SWAT are directly related to channel width at water level, which is affected by bankfull channel width (Eq. 3 and 5). Under scenarios 2-6, channel evaporation was in the range 0.28-0.41 m^3/s, while it was 1.32 m^3/s with M_0. This is not surprising considering the bankfull channel width values were smaller under scenario 2-6 compared to M_0. However, the implications for simulated water yield were negligeable since we found no sensitivity of streamflow over/underestimation to bankfull channel width representation. Under the Muskingum routing method, the total water storage in the channel is a sum of prism and wedge storages, which are affected by the rates of inflow and outflow (Neitsch et al., 2011). Although channel geometry representation had no influence on the watershed’s water budget, the changes provoked on flow rates may have underlying implications for channel routing. Studies such as Her et al. (2017) and Kim et al. (2022) have also shown modest impacts of channel width representation on simulated streamflow with SWAT. The impacts on streamflow simulation might have been greater if the model was run at sub-daily (e.g., hourly) time step. To accomplish this, sub-daily weather data must be available. This is beyond the scope of the current study and should be addressed in a future effort. Our findings also point to the need for model calibration to get right answers for the right reasons.

The impacts of channel width on simulated 1-day maximum flows were significant and may help to explain the changes in NSE values when predicting daily streamflow. Overall, 1-day maximum flows increased 20% by using alternative sources of channel width in SWAT. This is not surprising considering that under scenarios 2-6, the width of the channels was much smaller compared to the baseline model, which resonated in smaller cross-sectional area (Eq. 4), and thus higher flow rates (Eq. 6) and velocity (Eq. 7). Channel peak flow rate is simulated in SWAT as a function of average flow rate and a peak rate adjustment factor (Neitsch et al., 2011). As a result, increased flow rate stemming from reduced channel width has most likely increased peak flow rate, which in turn compounded the model overestimation of peak flows and impacted NSE values. It is worth noting that SWAT overestimated streamflow by 38% across the ACT river basin. Results suggest that enhancing the representation of channel width in SWAT can help improve model performance in watersheds where streamflow, especially peak flow, is underestimated. Additionally, the agreement between simulated and observed 1-day maximum flow improved at ten locations across the ACT river basin by using channel width estimates from M_{Ssts}, $M_{SstsReg}$, M_{GRWL}, M_{Emp}, and M_{Lidar}. Studies such as Han et al. (2019) have also shown better performance in capturing peak flows in SWAT by improving channel width representation. These results are particularly relevant considering the ecological implications of maximum flows, as well as their importance for watershed management and planning. For instance, maximum flows influence water resources management structures such as reservoirs through the opening of emergency spillways, and flood control in urban areas through the design of culverts and infiltration trenches. Additionally, maximum flows have ecological importance for ecosystem health (Kiesel et al., 2017; Richter et al., 1996). Maximum flows of various durations can modify the channel morphology as they shape the channel and therefore alter physical habitat conditions. For instance, fish species of ecologic, economic, and cultural relevance for Alabama such as largemouth bass and darters thrive in slow- and swift-flowing waters, respectively (Atkins et al., 2004). Maximum flows can also impact aquatic species because they influence spawning and population dynamics as they move to islands and/or floodplains during flooding events (Richter et al., 1996).

We used stream temperature as a surrogate to examine the impacts of channel width on water quality modeling in SWAT. To accomplish this, we used a recently developed physically-based equilibrium model to simulate water temperature with SWAT (Du et al., 2018). Our results demonstrate that daily stream temperatures predicted with M_{Ssts}, $M_{SstsReg}$, M_{GRWL}, M_{Emp}, M_{Lidar} were lower than default SWAT. Additionally, default SWAT overestimated observed stream temperature by over 5%, which was reduced to 2% under the alternative approaches. $M_{SstsReg}$ showed the smallest overestimation (0.7%) among all scenarios, which may be explained by the fact that the width of all channels was modified under $M_{SstsReg}$, which potentially resulted in bigger cumulative impacts. Lower stream temperature under scenarios 2-6 are most likely due to the slightly increased streamflow rates and decreased water yield predicted by these models. As shown by equation 9, the equilibrium stream temperature approach is directly affected by streamflow and total water yield, which are in turn affected by bankfull channel width and depth. Additionally, the change in stream temperature caused by heat transfer is influenced by the water travel time in the channel. Thus, our findings indicate that channel geometry has indirect, yet important, implications for stream temperature predictions. Additionally, the model performance in simulating daily stream temperature in terms of NSE was also enhanced under M_{Ssts}, $M_{SstsReg}$, M_{GRWL}, M_{Emp}, and M_{Lidar}. Considering that simulated stream temperature influences chemical reaction rates and dissolved oxygen saturation in SWAT (Neitsch et al., 2011), our findings suggest that more accurately representing channel width in SWAT may be beneficial for water quality applications. Although simulated stream temperature was affected by channel width representation in the current study, it is worth highlighting that here we rely on the physically based equilibrium model. Under the default stream temperature model in SWAT, which is solely a function of air temperature, our results showed no sensitivity of water temperature simulations to channel width. The relevance of better predicting stream temperature is justified by its ecological importance. Stream water temperature is an important regulator of aquatic life with direct (e.g., species reproduction, distribution, and migration) and indirect (water conductivity, salinity, pH, dissolved oxygen concentration) effects on the health and productivity of aquatic ecosystems (Ficklin et al., 2012). With underlying impacts on chemical and physical properties of waterbodies, stream temperature constitutes an important water quality variable for assessing aquatic biodiversity and freshwater ecosystem health (Du et al., 2018; Zhu et al., 2018, p. 2). Additionally, aquatic species such as fishes have specific thresholds of water temperature that they can tolerate and under which they thrive (Caissie et al., 2007). Fluctuations in the optimal water temperature ranges of a given species can negatively impact their habitat, dynamics, and population distributions in the stream (Du et al., 2019). Moreover, the growth rate and development of aquatic biota is highly influenced by water temperature. Other riverine processes such as nutrient cycling, decomposition, and degradation of organic matter are also influenced by water temperatures (Friberg et al., 2009).

We found significant sensitivities of sediment, nitrate, and phosphate loading simulations to channel width representation in SWAT. While the alternative data sources led to increased sediment loadings compared to the default model, the contrary was found for nitrate and phosphate. Sediment loadings were particularly affected, with percent increases ranging from 109 to 118% compared to the default model. This is most likely because SWAT uses the Modified Universal Soil Loss Equation (MUSLE) (Williams, 1975) to compute sediment yield. MUSLE predicts sediment loading based on peak runoff rate, which was significantly increased under the alternative channel width representations.

Our study has limitations and results must be interpreted with caution. For instance, channel width measurement with satellite imagery has inherent uncertainties associated with it (Allen and Pavelsky, 2015; Biron et al., 2013; Pavelsky and Smith, 2008; Zheng et al., 2018). Also, our approach in deriving bankfull widths from Streamstats considered a single background imagery, which may not completely reflect bankfull conditions as channel morphology presents seasonal fluctuations (Magliulo et al., 2021). Similarly, we derived bankfull channel widths at specific locations, which may not capture variations in channel width along a stream segment. To consider this uncertainty, we used a quantitative approach to estimate the variability in bankfull channel width along 5 km of the Alabama river. We found a standard deviation of 19 meters and average value of 257 meters, indicating a small variation. Additionally, channel width estimates from GRWL could only be derived for a few channels because of the coarser resolution of this dataset. Furthermore, although SWAT has the flexibility to allow users to modify channel widths, a fixed value is used for each channel, which may not reflect real world conditions. Even though our findings are relevant as they revealed that SWAT, a widely used watershed model, may misrepresent channel width when using the default values defined by the ArcSWAT program. Moreover, we showed the implications for hydrologic predictions brought about the representation of channel geometry in SWAT. More importantly, our study shows that site-specific bankfull channel width data exists either directly (e.g., estimates from global databases and LiDAR) or indirectly (e.g., aerial measurements) and can be used to enhance watershed modeling. Our proposed approaches are simple and may be replicated to other watersheds with different hydrologic conditions. Global datasets such as GRWL are extremely valuable information that can be leveraged in poorly monitored regions of the world. Also, the similar results generated under M_{Ssts} and $M_{SstsReg}$ indicate the feasibility of developing relationships between drainage area and channel width at major river sites and then extrapolate the empirical relationship to nearby locations. This is further confirmed by M_{Emp}, which despite relying on an empirical model developed for the Coastal Plain region, was applied to adjacent physiographic regions (Figure 1) and produced similar results to the other scenarios. Also, bankfull channel widths derived from high-resolution LiDAR data showed good agreement with the other alternative data sources. Overall, LiDAR-based bankfull channel width was 14% wider than the other sources. Although our study is in the context of the ACT river basin, our methodology can be applied to other study areas since most of the data sources utilized here are not region-specific. For instance, GRWL is readily available in vector format for the entire globe. Similarly, LiDAR information is becoming more popular and witnessing increased availability worldwide. Also, aerial imagery techniques relying on software such as Google Earth can be applied to any region of the Earth. The proposed methodology requires modelers to compile channel width data to regions outside our study area or located in different physiographic regions. However, the study domain comprises five distinct physiographic regions (Figure 1) spanning across the states Alabama, Georgia, and Tennessee and is comprised of several watersheds (Figure 1). This makes our results generalizable to a wide geographic range of diverse land-use distributions, soil types, elevation profiles, and hydrological conditions across the southeast United States. Finally, it is important to highlight that although we used the SWAT model, other popular watershed-scale hydrologic models such as HSPF, NWM, and MGB are based on similar assumptions. Thus, our findings can broadly serve the modeling community.

5. Summary and Conclusions

This study assessed the reliability of a widely used watershed model, SWAT, in representing bankfull channel width using values defined by ArcSWAT. We compared the default channel width values against five alternative data sources and measured values across the study area. Results indicate that the default regression equation used by ArcSWAT misrepresented bankfull channel width in the tested watershed system. The methodology was tested in a large watershed in Alabama, the Alabama-Coosa-Tallapoosa river basin, which has regional ecologic and economic relevance. The implications for streamflow, 1-day maximum flow, stream temperature, sediment and nutrient loading simulations were examined through a series of modeling experiments, each relying on a different source of channel width data. Our findings indicate no relevant changes in the amount of water flowing through the channel. However, the model performance measured with NSE significantly changed under the alternative approaches. The impacts on simulated maximum flows were substantial, with an average 20% increase in 1-day maximum flow found with the alternative sources of channel width. Similarly, stream temperature was affected by channel width representation, with lower temperatures simulated under the proposed scenarios. The default representation of channel width in SWAT led to overestimation of daily stream temperature compared to observations across the study domain. The alternative sources of channel width reduced model overestimation of steam temperature and increased NSE values, leading to better agreement with observations. Sediment loading increased by as much as 118% under the alternative sources of channel width, whilst nitrate and phosphate loadings decreased relative to the default model, with percent decreases as high as 8.3 and 18.8%, respectively.

Our study is the first to consistently demonstrate the limitations of channel width representation in current watershed modeling and the potential implications for hydrology and water quality. Overall, our findings indicate that bankfull channel width has important impacts on flow rate, especially peak flows. On the other hand, channel width representation has no impact on the amount of water flowing through the channel and is thus not critical for water balance computation. Bankfull channel width had important impacts on simulated stream temperature, sediment, and nutrient loadings, suggesting that channel width should be considered in water quality applications. Our study demonstrates that existent datasets and approaches such as aerial measurements, regional curves, LiDAR technology, and global databases can be incorporated in watershed models to improve our knowledge of the physical system. We observed a lack of field measurements of bankfull width and depth, and we postulate that these important hydrologic and hydraulic variables deserve more attention in field surveys. Approaches such as citizen-science, for instance, could be leveraged to increase the availability of field-measured bankfull channel width and depth data. Finally, our methodology is simple and may be replicated to other study regions, which makes our findings broadly available to the modeling community.

Acknowledgements

This paper is a result of research funded by the National Oceanic and Atmospheric Administration's RESTORE Science Program under award NA19NOS4510194 to Auburn University.

References

Abatzoglou, J.T., 2013. Development of gridded surface meteorological data for ecological applications and modelling. International Journal of Climatology 33, 121–131. https://doi.org/10.1002/joc.3413

Abbaspour, K.C., Rouholahnejad, E., Vaghefi, S., Srinivasan, R., Yang, H., Kløve, B., 2015. A continental-scale hydrology and water quality model for Europe: Calibration and uncertainty of a high-resolution large-scale SWAT model. Journal of Hydrology 524, 733–752. https://doi.org/10.1016/j.jhydrol.2015.03.027

Allen, G.H., Pavelsky, T.M., 2018. Global extent of rivers and streams. Science 361, 585–588. https://doi.org/10.1126/science.aat0636

Allen, G.H., Pavelsky, T.M., 2015. Patterns of river width and surface area revealed by the satellite-derived North American River Width data set. Geophysical Research Letters 42, 395–402. https://doi.org/10.1002/2014GL062764

Allen, P.M., Arnold, J.C., Byars, B.W., 1994. Downstream Channel Geometry for Use in Planning-Level Models1. JAWRA Journal of the American Water Resources Association 30, 663–671. https://doi.org/10.1111/j.1752-1688.1994.tb03321.x

Ames, D.P., Rafn, E.B., Van Kirk, R., Crosby, B., 2009. Estimation of stream channel geometry in Idaho using GIS-derived watershed characteristics. Environmental Modelling & Software 24, 444–448. https://doi.org/10.1016/j.envsoft.2008.08.008

Arnold, J.G., Srinivasan, R., Muttiah, R.S., Williams, J.R., 1998. Large Area Hydrologic Modeling and Assessment Part I: Model Development1. JAWRA Journal of the American Water Resources Association 34, 73–89. https://doi.org/10.1111/j.1752-1688.1998.tb05961.x

Atkins, J.B., Zappia, H., Robinson, J.L., McPherson, A.K., Moreland, R.S., Harned, D.A., Johnston, B.F., Harvill, J.S., 2004. Water quality in the Mobile River Basin, Alabama, Georgia, Mississippi, and Tennessee, 1999-2001 (USGS Numbered Series No. 1231), Water quality in the Mobile River Basin, Alabama, Georgia, Mississippi, and Tennessee, 1999-2001, Circular. U.S. Geological Survey. https://doi.org/10.3133/cir1231

Baradei, S.E., 2020. Studying the Effect of Channel Geometry on Different Water Quality Variables for Effective Designs and Waste Allocation Plans for Waterways. Water 12, 2176. https://doi.org/10.3390/w12082176

Battin, A., Kinerson, R., Lahlou, M., 1998. EPA'S Better Assessment Science Integrating Point and Non-point Sources (BASINS) - A powerful tool for managing watersheds, in: Proc. GISHydro98. Presented at the Environmental Systems Research, Inc. Users Conference, July, San Diego, CA, pp. 27–31.

Bicknell, B.R., Imhoff, J.C., Kittle, J.L., Donigian, A.S., Johanson, R.C., 2001. Hydrological Simulation Program--FORTRAN User's Manual for Version 11. USEPA, Athens, Georgia.

Bieger, K., Rathjens, H., Allen, P.M., Arnold, J.G., 2015. Development and Evaluation of Bankfull Hydraulic Geometry Relationships for the Physiographic Regions of the United States. JAWRA Journal of the American Water Resources Association 51, 842–858. https://doi.org/10.1111/jawr.12282

Biron, P.M., Choné, G., Buffin-Bélanger, T., Demers, S., Olsen, T., 2013. Improvement of streams hydro-geomorphological assessment using LiDAR DEMs. Earth Surface Processes and Landforms 38, 1808–1821. https://doi.org/10.1002/esp.3425

Bizzi, S., Piégay, H., Demarchi, L., Van de Bund, W., Weissteiner, C. j., Gob, F., 2019. LiDAR-based fluvial remote sensing to assess 50–100-year human-driven channel changes at a regional level: The case of the Piedmont Region, Italy. Earth Surface Processes and Landforms 44, 471–489. https://doi.org/10.1002/esp.4509

Blackard, J.A., Finco, M.V., Helmer, E.H., Holden, G.R., Hoppus, M.L., Jacobs, D.M., Lister, A.J., Moisen, G.G., Nelson, M.D., Riemann, R., Ruefenacht, B., Salajanu, D., Weyermann, D.L., Winterberger, K.C., Brandeis, T.J., Czaplewski, R.L., McRoberts, R.E., Patterson, P.L., Tymcio, R.P., 2008. Mapping U.S. forest biomass using nationwide forest inventory data and moderate resolution information. Remote Sensing of Environment, Remote Sensing Data Assimilation Special Issue 112, 1658–1677. https://doi.org/10.1016/j.rse.2007.08.021

Brackins, J., Moragoda, N., Rahman, A., Cohen, S., Lowry, C., 2021. The Role of Realistic Channel Geometry Representation in Hydrological Model Predictions. JAWRA Journal of the American Water Resources Association 57, 222–240. https://doi.org/10.1111/1752-1688.12865

Caissie, D., Satish, M.G., El-Jabi, N., 2007. Predicting water temperatures using a deterministic model: Application on Miramichi River catchments (New Brunswick, Canada). Journal of Hydrology 336, 303–315. https://doi.org/10.1016/j.jhydrol.2007.01.008

Choi, B., Kang, H., Lee, W.H., 2018. Baseflow Contribution to Streamflow and Aquatic Habitats Using Physical Habitat Simulations. Water 10, 1304. https://doi.org/10.3390/w10101304

Clark, M.P., Nijssen, B., Lundquist, J.D., Kavetski, D., Rupp, D.E., Woods, R.A., Freer, J.E., Gutmann, E.D., Wood, A.W., Brekke, L.D., Arnold, J.R., Gochis, D.J., Rasmussen, R.M., 2015. A unified approach for process-based hydrologic modeling: 1. Modeling concept. Water Resources Research 51, 2498–2514. https://doi.org/10.1002/2015WR017198

Cunge, J.A., 1969. On The Subject Of A Flood Propagation Computation Method (Musklngum Method). Journal of Hydraulic Research 7, 205–230. https://doi.org/10.1080/00221686909500264

De Cicco, L.A., Hirsch, R.M., Lorenz, D., Watkins, D., 2018. dataRetrieval. U.S. Geological Survey. https://doi.org/10.5066/P9X4L3GE

Devia, G.K., Ganasri, B.P., Dwarakish, G.S., 2015. A Review on Hydrological Models. Aquatic Procedia, INTERNATIONAL CONFERENCE ON WATER RESOURCES, COASTAL AND OCEAN ENGINEERING (ICWRCOE'15) 4, 1001–1007. https://doi.org/10.1016/j.aqpro.2015.02.126

Doll, B.A., Wise-Frederick, D.E., Buckner, C.M., Wilkerson, S.D., Harman, W.A., Smith, R.E., Spooner, J., 2002. Hydraulic Geometry Relationships for Urban Streams Throughout the Piedmont of North Carolina1. JAWRA Journal of the American Water Resources Association 38, 641–651. https://doi.org/10.1111/j.1752-1688.2002.tb00986.x

Du, X., Shrestha, N.K., Ficklin, D.L., Wang, J., 2018. Incorporation of the equilibrium temperature approach in a Soil and Water Assessment Tool hydroclimatological stream temperature model. Hydrology and Earth System Sciences 22, 2343–2357. https://doi.org/10.5194/hess-22-2343-2018

Du, X., Shrestha, N.K., Wang, J., 2019. Assessing climate change impacts on stream temperature in the Athabasca River Basin using SWAT equilibrium temperature model and its potential impacts on stream ecosystem. Science of The Total Environment 650, 1872–1881. https://doi.org/10.1016/j.scitotenv.2018.09.344

Elosegi, A., Díez, J., Mutz, M., 2010. Effects of hydromorphological integrity on biodiversity and functioning of river ecosystems. Hydrobiologia 657, 199–215. https://doi.org/10.1007/s10750-009-0083-4

Ficklin, D.L., Luo, Y., Stewart, I.T., Maurer, E.P., 2012. Development and application of a hydroclimatological stream temperature model within the Soil and Water Assessment Tool. Water Resources Research 48. https://doi.org/10.1029/2011WR011256

Fisher, G.B., Bookhagen, B., Amos, C.B., 2013. Channel planform geometry and slopes from freely available high-spatial resolution imagery and DEM fusion: Implications for channel width scalings, erosion proxies, and fluvial signatures in tectonically active landscapes. Geomorphology 194, 46–56. https://doi.org/10.1016/j.geomorph.2013.04.011

Friberg, N., Dybkjær, J.B., Olafsson, J.S., Gislason, G.M., Larsen, S.E., Lauridsen, T.L., 2009. Relationships between structure and function in streams contrasting in temperature. Freshwater Biology 54, 2051–2068. https://doi.org/10.1111/j.1365-2427.2009.02234.x

Gochis, D.J., Dugger, A., McCreight, J., Karsten, L.R., Logan, Y.W., Pan, L., Cosgrove, B., 2016. Technical Description of the National Water Model Implementation of WRF-Hydro. Technical Report. Technical Repor.

Goetz, S., Fiske, G., 2008. Linking the diversity and abundance of stream biota to landscapes in the mid-Atlantic USA. Remote Sensing of Environment, Applications of Remote Sensing to Monitoring Freshwater and Estuarine Systems 112, 4075–4085. https://doi.org/10.1016/j.rse.2008.01.023

Gorelick, N., Hancher, M., Dixon, M., Ilyushchenko, S., Thau, D., Moore, R., 2017. Google Earth Engine: Planetary-scale geospatial analysis for everyone. Remote Sensing of Environment, Big Remotely Sensed Data: tools, applications and experiences 202, 18–27. https://doi.org/10.1016/j.rse.2017.06.031

Guswa, A.J., Brauman, K.A., Brown, C., Hamel, P., Keeler, B.L., Sayre, S.S., 2014. Ecosystem services: Challenges and opportunities for hydrologic modeling to support decision making. Water Resources Research 50, 4535–4544. https://doi.org/10.1002/2014WR015497

Haas, H., Reaver, N.G.F., Karki, R., Kalin, L., Srivastava, P., Kaplan, D.A., Gonzalez-Benecke, C., 2021. Improving the representation of forests in hydrological models. Science of The Total Environment 151425. https://doi.org/10.1016/j.scitotenv.2021.151425

Hall, C.A., Saia, S.M., Popp, A.L., Dogulu, N., Schymanski, S.J., Drost, N., van Emmerik, T., Hut, R., 2022. A hydrologist's guide to open science. Hydrology and Earth System Sciences 26, 647–664. https://doi.org/10.5194/hess-26-647-2022

Han, J., Lee, D., Lee, S., Chung, S.-W., Kim, S.J., Park, M., Lim, K.J., Kim, J., 2019. Evaluation of the Effect of Channel Geometry on Streamflow and Water Quality Modeling and Modification of Channel Geometry Module in SWAT: A Case Study of the Andong Dam Watershed. Water 11, 718. https://doi.org/10.3390/w11040718

Her, Y., Jeong, J., Bieger, K., Rathjens, H., Arnold, J., Srinivasan, R., 2017. Implications of Conceptual Channel Representation on SWAT Streamflow and Sediment Modeling. JAWRA Journal of the American Water Resources Association 53, 725–747. https://doi.org/10.1111/1752-1688.12533

Jardim, P., Fleischmann, A.S., Coelho, V.R., Oliveira, A.M., Pelinson, D., Passaia, O., Colossi, B.R., Pontes, P.R.M., Siqueira, V.A., Fan, F.M., Collischon, W., 2017. MGB-IPH application example manual using IPH-Hydro Tools. Instituto de Pesquisas Hidraulicas, Universidade Federal do Rio Grande do Sul.

Johnson, G.C., Kidd, R.E., Journey, C.A., Zappia, H., Atkins, J.B., 2002. Environmental setting and water-quality issues of the Mobile River Basin, Alabama, Georgia, Mississippi, and Tennessee (USGS Numbered Series No. 2002–4162), Environmental setting and water-quality issues of the Mobile River Basin, Alabama, Georgia, Mississippi, and Tennessee, Water-Resources Investigations Report. https://doi.org/10.3133/wri024162

Johnson, P.A., Fecko, B.J., 2008. Regional channel geometry equations: a statistical comparison for physiographic provinces in the eastern US. River Research and Applications 24, 823–834. https://doi.org/10.1002/rra.1080

Kale, V.S., Hire, P.S., 2004. Effectiveness of monsoon floods on the Tapi River, India: role of channel geometry and hydrologic regime. Geomorphology 57, 275–291. https://doi.org/10.1016/S0169-555X(03)00107-7

Kiesel, J., Guse, B., Pfannerstill, M., Kakouei, K., Jähnig, S.C., Fohrer, N., 2017. Improving hydrological model optimization for riverine species. Ecological Indicators 80, 376–385. https://doi.org/10.1016/j.ecolind.2017.04.032

Kim, D.-W., Chung, E.G., Kim, K., Kim, Y., 2022. Impact of riverbed topography on hydrology in small watersheds using Soil and Water Assessment Tool. Environmental Modelling & Software 152, 105383. https://doi.org/10.1016/j.envsoft.2022.105383

Leckie, D., Cloney, E., Jay, C., Paradine, D., 2005. Automated Mapping of Stream Features with High-Resolution Multispectral Imagery: An Example of the Capabilities. Photogrammetric Engineering & Remote Sensing 71, 145–155. https://doi.org/10.14358/PERS.71.2.145

Lenat, D.R., Crawford, J.K., 1994. Effects of land use on water quality and aquatic biota of three North Carolina Piedmont streams. Hydrobiologia 294, 185–199. https://doi.org/10.1007/BF00021291

Leopold, L.B., Maddock Jr., T., 1953. The hydraulic geometry of stream channels and some physiographic implications (USGS Numbered Series No. 252), The hydraulic geometry of stream channels and some physiographic implications, Professional Paper. U.S. Government Printing Office, Washington, D.C. https://doi.org/10.3133/pp252

Mac Nally, R., Wallis, E., Lake, P.S., 2011. Geometry of biodiversity patterning: assemblages of benthic macroinvertebrates at tributary confluences. Aquat Ecol 45, 43–54. https://doi.org/10.1007/s10452-010-9322-z

Magliulo, P., Cusano, A., Giannini, A., Sessa, S., Russo, F., 2021. Channel Width Variation Phases of the Major Rivers of the Campania Region (Southern Italy) over 150 Years: Preliminary Results. Earth 2, 374–386. https://doi.org/10.3390/earth2030022

McKean, J., Nagel, D., Tonina, D., Bailey, P., Wright, C.W., Bohn, C., Nayegandhi, A., 2009. Remote Sensing of Channels and Riparian Zones with a Narrow-Beam Aquatic-Terrestrial LIDAR. Remote Sensing 1, 1065–1096. https://doi.org/10.3390/rs1041065

McLaughlin, D.L., Kaplan, D.A., Cohen, M.J., 2013. Managing Forests for Increased Regional Water Yield in the Southeastern U.S. Coastal Plain. JAWRA Journal of the American Water Resources Association 49, 953–965. https://doi.org/10.1111/jawr.12073

Michalková, M., Piégay, H., Kondolf, G. m., Greco, S. e., 2011. Lateral erosion of the Sacramento River, California (1942–1999), and responses of channel and floodplain lake to human influences. Earth Surface Processes and Landforms 36, 257–272. https://doi.org/10.1002/esp.2106

Monteith, J.L., 1965. Evaporation and environment. Symposia of the Society for Experimental Biology 19, 205–234.

Moriasi, D.N., Arnold, J.G., Liew, M.W.V., Bingner, R.L., Harmel, R.D., Veith, T.L., 2007. Model evaluation guidelines for systematic quantification of accuracy in watershed simulations.

Moriasi, D.N., Gitau, M.W., Pai, N., Daggupati, P., 2015. Hydrologic and Water Quality Models: Performance Measures and Evaluation Criteria.

Mu, Q., Zhao, M., Running, S.W., 2013. MODIS Global Terrestrial Evapotranspiration (ET) Product (NASE MOD16A2/A3). Algorithm Theoretical Basis Document, Collectio, 5, 600.

Muttiah, R., Srinivasan, R., Allen, P., 2007. Prediction of two-year peak stream discharges using neural networks. JAWRA Journal of the American Water Resources Association 33, 625–630. https://doi.org/10.1111/j.1752-1688.1997.tb03537.x

Neitsch, S.L., Arnold, J.G., Kiniry, J.R., Williams, J.R., 2011. Soil and water assessment tool theoretical documentation: version 2009. Texas Water Resources Institute Technical Report No. 406. Texas Water Resources Institute, USA.

Passalacqua, P., Do Trung, T., Foufoula-Georgiou, E., Sapiro, G., Dietrich, W.E., 2010. A geometric framework for channel network extraction from lidar: Nonlinear diffusion and geodesic paths. Journal of Geophysical Research: Earth Surface 115. https://doi.org/10.1029/2009JF001254

Pavelsky, T.M., Smith, L.C., 2008. RivWidth: A Software Tool for the Calculation of River Widths From Remotely Sensed Imagery. IEEE Geoscience and Remote Sensing Letters 5, 70–73. https://doi.org/10.1109/LGRS.2007.908305

Richter, B.D., Baumgartner, J.V., Powell, J., Braun, D.P., 1996. A Method for Assessing Hydrologic Alteration within Ecosystems. Conservation Biology 10, 1163–1174. https://doi.org/10.1046/j.1523-1739.1996.10041163.x

Rodrigues, A.M., Quintino, V., Sampaio, L., Freitas, R., Neves, R., 2011. Benthic biodiversity patterns in Ria de Aveiro, Western Portugal: Environmental-biological relationships. Estuarine, Coastal and Shelf Science 95, 338–348. https://doi.org/10.1016/j.ecss.2011.05.019

Scanlon, B.R., Zhang, Z., Save, H., Sun, A.Y., Müller Schmied, H., van Beek, L.P.H., Wiese, D.N., Wada, Y., Long, D., Reedy, R.C., Longuevergne, L., Döll, P., Bierkens, M.F.P., 2018. Global models underestimate large decadal declining and rising water storage trends relative to GRACE satellite data. Proceedings of the National Academy of Sciences 115, E1080–E1089. https://doi.org/10.1073/pnas.1704665115

Sharpley, A., Jarvie, H.P., Buda, A., May, L., Spears, B., Kleinman, P., 2013. Phosphorus Legacy: Overcoming the Effects of Past Management Practices to Mitigate Future Water Quality Impairment. Journal of Environmental Quality 42, 1308–1326. https://doi.org/10.2134/jeq2013.03.0098

Shatnawi, F.M., Goodall, J.L., 2010. Comparison of Flood Top Width Predictions Using Surveyed and LiDAR-Derived Channel Geometries. Journal of Hydrologic Engineering 15, 97–106. https://doi.org/10.1061/(ASCE)HE.1943-5584.0000161

Siqueira, V., Fleischmann, A., Jardim, P., Fan, F., Collischonn, W., 2016. IPH-Hydro Tools: a GIS coupled tool for watershed topology acquisition in an open-source environment. RBRH 21, 274–287. https://doi.org/10.21168/rbrh.v21n1.p274-287

Stagge, J.H., Rosenberg, D.E., Abdallah, A.M., Akbar, H., Attallah, N.A., James, R., 2019. Assessing data availability and research reproducibility in hydrology and water resources. Sci Data 6, 190030. https://doi.org/10.1038/sdata.2019.30

Stewardson, M., 2005. Hydraulic geometry of stream reaches. Journal of Hydrology 306, 97–111. https://doi.org/10.1016/j.jhydrol.2004.09.004

US Army Corps of Engineers, 2023. HEC-RAS River Analysis System. (User Manual), HEC-RAS Release Notes. Hydrologic Engineering Center.

Utz, R.M., Hilderbrand, R.H., Boward, D.M., 2009. Identifying regional differences in threshold responses of aquatic invertebrates to land cover gradients. Ecological Indicators 9, 556–567. https://doi.org/10.1016/j.ecolind.2008.08.008

Williams, J.J.R., 1975. Sediment-yield prediction with Universal Equation using runoff energy factor [WWW Document]. URL /paper/Sediment-yield-prediction-with-Universal-Equation-Williams/a9bc4612310f980c973575cbf86c63b77a01ace1 (accessed 7.18.20).

Winterbottom, S.J., Gilvear, D.J., 1997. Quantification of channel bed morphology in gravel-bed rivers using airborne multispectral imagery and aerial photography. Regulated Rivers: Research & Management 13, 489–499. https://doi.org/10.1002/(SICI)1099-1646(199711/12)13:6<489::AID-RRR471>3.0.CO;2-X

Yamazaki, D., O'Loughlin, F., Trigg, M.A., Miller, Z.F., Pavelsky, T.M., Bates, P.D., 2014. Development of the Global Width Database for Large Rivers. Water Resources Research 50, 3467–3480. https://doi.org/10.1002/2013WR014664

Yang, X., Pavelsky, T.M., Allen, G.H., Donchyts, G., 2020. RivWidthCloud: An Automated Google Earth Engine Algorithm for River Width Extraction From Remotely Sensed Imagery. IEEE Geoscience and Remote Sensing Letters 17, 217–221. https://doi.org/10.1109/LGRS.2019.2920225

Yen, H., Bailey, R.T., Arabi, M., Ahmadi, M., White, M.J., Arnold, J.G., 2014. The Role of Interior Watershed Processes in Improving Parameter Estimation and Performance of Watershed Models. Journal of Environment Quality 43, 1601. https://doi.org/10.2134/jeq2013.03.0110

Zema, D.A., Bombino, G., Denisi, P., Lucas-Borja, M.E., Zimbone, S.M., 2018. Evaluating the effects of check dams on channel geometry, bed sediment size and riparian vegetation in Mediterranean mountain torrents. Science of The Total Environment 642, 327–340. https://doi.org/10.1016/j.scitotenv.2018.06.035

Zheng, X., Tarboton, D.G., Maidment, D.R., Liu, Y.Y., Passalacqua, P., 2018. River Channel Geometry and Rating Curve Estimation Using Height above the Nearest Drainage. JAWRA Journal of the American Water Resources Association 54, 785–806. https://doi.org/10.1111/1752-1688.12661

Zhu, S., Du, X., Luo, W., 2018. Incorporation of the simplified equilibrium temperature approach in a hydrodynamic and water quality model – CE-QUAL-W2. Water Supply 19, 156–164. https://doi.org/10.2166/ws.2018.063